CAPITAL UNIVERSITY OF SCIENCE AND TECHNOLOGY, ISLAMABAD

MHD Radiative Hybrid Nanofluid Flow with Inclined Magnetic Field

by

Mehwish Ibrahim

A thesis submitted in partial fulfillment for the degree of Master of Philosophy

in the

Faculty of Computing
Department of Mathematics

2022

*I dedicate my dissertation work to my **family** and dignified **teachers**. A special feeling of gratitude to my loving parents who have supported me in my studies.*

CERTIFICATE OF APPROVAL

MHD Radiative Hybrid Nanofluid Flow with Inclined Magnetic Field

by

Mehwish Ibrahim

(MMT191030)

THESIS EXAMINING COMMITTEE

(a)	External Examiner	Dr. Nabeela Kousar	AIR University, Islamabad
(b)	Internal Examiner	Dr. Muhammad Sabeel Khan	CUST, Islamabad
(c)	Supervisor	Dr. Dur-e-Shehwar Sagheer	CUST, Islamabad

Dr. Dur-e-Shehwar Sagheer
Thesis Supervisor
November, 2022

Dr. Muhammad Sagheer
Head
Dept. of Mathematics
November, 2022

Dr. M. Abdul Qadir
Dean
Faculty of Computing
November, 2022

Author's Declaration

I, **Mehwish Ibrahim**, hereby state that my MPhil thesis titled "**MHD Radiative Hybrid Nanofluid Flow with Inclined Magnetic Field**" is my own work and has not been submitted previously by me for taking any degree from Capital University of Science and Technology, Islamabad or anywhere else in the country/abroad.

At any time if my statement is found to be incorrect even after my graduation, the University has the right to withdraw my MPhil Degree.

(Mehwish Ibrahim)
Registration No: MMT191030

Plagiarism Undertaking

I solemnly declare that research work presented in this thesis titled "**MHD Radiative Hybrid Nanofluid Flow with Inclined Magnetic Field**" is solely my research work with no significant contribution from any other person. Small contribution/help wherever taken has been dully acknowledged and that complete thesis has been written by me.

I understand the zero tolerance policy of the HEC and Capital University of Science and Technology towards plagiarism. Therefore, I as an author of the above titled thesis declare that no portion of my thesis has been plagiarized and any material used as reference is properly referred/cited.

I undertake that if I am found guilty of any formal plagiarism in the above titled thesis even after award of MPhil Degree, the University reserves the right to withdraw/revoke my MPhil degree and that HEC and the University have the right to publish my name on the HEC/University website on which names of students are placed who submitted plagiarized work.

(Mehwish Ibrahim)
Registration No: MMT191030

Acknowledgement

I got no words to articulate my cordial sense of gratitude to **Almighty Allah** who is the most merciful and most beneficent to his creation.

I also express my gratitude to the last Prophet of **Almighty Allah, Prophet Muhammad (PBUH)** the supreme reformer of the world and knowledge for human being.

I would like to be thankful to all those who provided support and encouraged me during this work.

I would like to be grateful to my thesis supervisor **Dr. Dur-e-Shehwar Sagheer**, for guiding and encouraging towards writing this thesis. It would have remained incomplete without her endeavours. Due to her efforts I was able to write and complete this assertation. Also special thanks gives to **Dr. Muhammad Sagheer** for his valuable suggestions and co-operation. I would like to thanks all my teachers in department of mathematics.

I would like to pay great tribute to my **parents**, for their prayers, moral support, encouragment and appreciation.

Last but not the least, I want to express my gratitude to my **friends** and **brothers** specially **Tahseen Akhtar**, **Ghulam Abass**, **Ghulam Fareed** and **Naveed Ibrahim** who helped me throughout my MPhil degree.

(Mehwish Ibrahim)

Abstract

The effect of an inclined magnetic field on the flow of an electrically conducting hybrid nanofluid via a nonlinear stretching sheet through a porous media with frictional heating is investigated numerically in this work. The model of the flow problem is a system of PDEs. These partial differential equations are transformed into ordinary differential equation by the aid of similarity transformations. The shooting method is then used to numerically solve the reduced equations. The influence of physical parameters such as nanoparticle volume fraction, permeability parameter, nonlinear stretching sheet parameter, magnetic parameter, heat generation parameter, Prandtl number and radiation parameter on the velocity profile, temperature distribution, skin friction coefficient and Nusselt number are studied and presented in graphical and tabular forms. The findings show that increasing the nanoparticle volume fraction and permeability parameter increases the rate of heat transfer. The temperature distribution is also influenced by the presence of permeability parameter, magnetic parameter, Inclined magnetic angle and nanoparticle volume fraction. This demonstrates how heat transfer and nanofluid flow behaviours can be influenced by the volume fraction of nanoparticles.

Contents

List of Figures

List of Tables

Abbreviations

IVPs	Initial value problems
MHD	Magnetohydrodynamics
ODEs	Ordineary differential equations
PDEs	Partial differential equations
RK	Runge-Kutta

Symbols

μ	Viscosity
ρ	Density
ν	Kinematic viscosity
τ	Stress tensor
k	Thermal conductivity
σ	Electrical conductivity
u	x-component of fluid velocity
v	y-component of fluid velocity
B_0	Magnetic field constant
k_0	Permeability constant
a	Stretching constant
T_w	Temperature of the wall
T_∞	Ambient temperature of the nanofluid
T	Temperature
ρ_f	Density of the fluid
ν_f	Kinematic viscosity of the base fluid
ρ_{nf}	Density of the nanofluid
μ_{nf}	Viscosity of the nanofluid
q_r	Radiative heat flux
q	Heat generation constant
q_w	Heat flux
σ^*	Stefan Boltzmann constant
k^*	Absorption coefficient

ψ	Stream function
ξ	Similarity variable
C_f	Skin friction coefficient
Nu	Nusselt number
Nu_x	Local Nusselt number
Re	Reynolds number
Re_x	Local Reynolds number
ϕ	Nanoparticle volume fraction
R	Thermal radiation parameter
n	Stretching parameter
M	Magnetic parameter
K	Permeability parameter
Ec	Eckert number
Pr	Prandtl number
Q	Heat generation parameter
ρ_s	Density of nanoparticle
μ_f	Viscosity of the base fluid
$(\rho C_p)_f$	Heat capacitance of base fluid
$(\rho C_p)_s$	Heat capacitance of nanoparticle
σ_f	Electrical conductivity of the base fluid
σ_s	Electrical conductivity of the nanoparticle
k_f	Thermal conductivity of the base fluid
k_s	Thermal conductivity of the nanoparticle
f	Dimensionless velocity
θ	Dimensionless temperature
h	Dimensionless concentration
β_f	Thermal expansion coefficient of fluid
β_s	Thermal expansion coefficient of nanoparticle
α	Thermal diffisuitivity of hybrid nanofluid
ρ_{hnf}	Density of hybrid nanofluid
μ_{hnf}	Viscosity of hybrid nanofluid

k_{hnf}	Thermal conductivity of hybrid nanofluid
$(\rho C_p)_{s1}$	Heat capacitance of titanium particle
$(\rho C_p)_{s2}$	Heat capacitance of copper particle
$(\rho C_p)_{hnf}$	Heat capacitance of hybrid nanofluid

Chapter 1

Introduction

In reaction to an applied external force, a phase of matter known as a fluid, flows or deforms. Fluids come in three different forms: liquids, gases, and plasma [1]. It is a material that has vanishing shear modulus or to put it another way, a material that cannot tolerate any applied shear force. Since fluid is essential for life and is important to many natural processes, the researchers from all around the world are attempting to learn more about how fluids move. We analyse fluid flow and how forces affect fluid movement in the area of fluid dynamics, a subfield of fluid mechanics. It provides methods for understanding how the stars, the ocean, the current, the tectonic plate, and the blood flow have evolved [2]. Archimedes is credited for creating the Archimedes principle, which deals with the motion of objects. The static behaviour of fluids is a fundamental premise of fluid dynamics.

Fluids can be further classified as Newtonian or non-Newtonian fluids depending on the relationship between two physical parameters, specifically the relationship between stress and strain. Non-Newtonian fluids are those that do not exhibit a linear correlation between the shear stress and the rate of deformation. In other terms, non-Newtonian fluids are fluids that contradict Newton's viscosity law. Blood, Ketchup, paint, shampoo, muck, and other liquids behave in ways that are not Newtonian. Non-Newtonian fluid is used in many different industries, such as oil recovery, filtration, polymer engineering, ceramic production, and petroleum

production. In addition, it is crucial for the heating of geothermal energy, the disposal of nuclear waste, and the construction of oil reservoirs [3].

Choi [4] initially used the term "nanofluid" to describe a new form of fluid. Nanofluid is a blend of conventional low thermal conductivity fluid with nanoparticles with a size smaller than 100 nm. It can also be defined as "Tinny size particles suspended in a base fluid are known as nanofluids". The most commonly in use nanoparticles are carbon nanotubes, carbides, metals, or oxides nanofluids. These fluids are created synthetically to have better thermal conductivity than any basic fluids. The thermal conductivity of nanofluids can be boosted by adding gold, copper, silver, and other nanoparticles to the base fluid. Buongiorno [5] studied the element that increased the thermal conductivity of nanofluids. He noticed that a change in the fluid's thermal conductivity is caused by both the thermophoresis effect and Brownian motion. In the heavy vehicle and information technology industries, nanofluid can also be utilised as a coolant. In many industrial, biomedical, and technical domains, nanofluid is a blessing.

In 2007, Tiwari and Das [6] created a model to examine heat and nanofluid transport in a square cavity driven by a two-sided lid and examined the impact of nanoparticle volume percentage. They focused on how important nanoparticle volume fraction is for determining the effect of nanoparticles on fluid flow and the rate of heat transfer. According to Yang et al. [7], the volume proportion of nanoparticles and their various characteristics, such as diameter and shape, have a significant impact on the thermal conductivity of nanofluid.
Khan and Pop [8] were the first to do an experiment utilising Buongiorno's setup that showed how nanofluid flow behaved over a stretching sheet. They got to the conclusion that as the Brownain diffusion and thermophoresis parameters are raised, the rate of heat transfer decreases. Khan and Pops [8] original experiment was slightly modified over time by Rana and Bhargava [9]. Using the finite element method, they concentrated on the steady flow of a viscous nanofluid over a nonlinear stretching sheet. The thickness of the thermal boundary layer was found to

be improved by increasing the Brownain motion and thermophoresis parameters, according to their research.

Magnetohydrodynamics is a branch of mechanics that examines conduction fluid flow in the presence of an external magnetic field. Alfen [10], a Swedish scientist, was the first to describe the MHD fluid. The petroleum industry, MHD power generators, crystal formation, etc. are just a few engineering scenarios where MHD fluid flow through a heated surface has numerous critical applications. The MHD natural convection flow of spinning fluid through a porous sheet was studied by Mbeledogu and Ogulu [11]. They also studied the effects of radiation and heat transport. Through MHD, the boundary layer structure can be altered, improving fluid flow in a particular direction. Several industrial operations, such as the production of materials and metal casting, depend heavily on the application of an external magnetic field. Chauhan and Agrawal [12] conducted an analysis of the MHD flow and heat transfer across a channel employing a permeable sheet. They discovered that two variables, such as the magnetic number and suction parameter, can control the cooling rate. They discovered that the magnetic number and the suction parameter, respectively, can control the rate of cooling. Eftekhari and Moradi used a vertical plate filled with nanofluid to illustrate the 2D mixed convection MHD boundary layer stagnation point flow in the presence of thermal radiation [13].

Numerous novel and anticipated studies on common electrically conducting flows demonstrate that the introduction of a magnetic field dramatically changes their heat transfer and transit characteristics. Heat transfer efficiency depends on how well operating fluids like water (H_2O), titanium dioxide (TiO_2), copper (Cu) and ethyl glycol $(CH_2OH)_2$ carry heat. As a continuation of their research on nanofluids, scientists have recently experimented with hybrid nanofluids, which are produced by suspending dissimilar nanoparticles in mixture or composite form. However, hybrid nanofluids represent a whole new class of nanofluid. In a nutshell, hybrid nanofluids can be created by suspending (i) various types of nanoparticles (two or more types) in base fluid and (ii) hybrid (composite) nanoparticles in

base fluid. In order to deliver these properties in a homogenous phase, a hybrid material must concurrently combine the physical and chemical properties of many materials [14]. In-depth literature on hybrid nanofluids, such as magnetised hybrid condensed nanofluid flow with radiation, hybrid nanofluid flow inside a microchannel, and hydrothermal characteristics of magnetised $TiO_2 - CoFe_2O_4$ water-based steady hybrid nanofluid flow, was described by Acharya et al. ([15], [16], [17]).

Considering its significance in the industrial processing of glass fibre, metal wires, polymer sheets, paper production, and plastic films, the evaluation of heat transfer across a boundary layer flow through a continuous stretched surface subject to the prescribed heat flux and surface temperature has attracted considerable interest. When making plastic and glass out of polymers, the cooling rate is greatly influenced by the characteristics of the final product. Radiation effect on MHD Casson fluid flow over an inclined non-linear surface with chemical reaction in a Forchheimer porous medium has been discussed in [18].

In the material processing, fuel cell equipment, drying operations, geothermal energy, dribbling bed chromatography, oil recovery, and many other processes, the flow across a porous media is extremely important. A proactive method to improve thermal performance is the combined effect of mass and heat transfer associated with the magnetohydrodynamic boundary layer flow of a nanofluid over a porous material. In this context, Chamkha et al. [19] looked at how a porous medium and natural convection affected the boundary layer flow across an inclined surface in terms of thermal radiation and uneven porosity. The average Nusselt number and the flow structure are significantly influenced by the permeability of the porous media, according to the mass and heat transfer experiment conducted by Hadidi et al. [20] through a porous inclined enclosure. The heat transmission in hybrid nanofluids over a stretching surface has been covered by S. U. Devi and S. A. Devi, [21]. The hybrid nanofluids have far higher thermal conductivities than nanofluids ($K_{hnf} \geq K_{nf}$), which contributes significantly to the improvement of heat transfer coefficients and leads to improved results in terms of decreased thermal energy loss and production costs [22], [23] and [24].

1.1 Contributions to the Thesis

In this research, a review study of [25] has been presented and then the flow analysis has been extended with MHD radiative hybrid nanofluid flow with inclined magnetic field. The main focus is to study the numerical analysis of MHD nanofluid flow via a nonlinear stretching sheet saturated in a porous medium in the presence of a inclined magnetic field, heat generation, and thermal radiation. Through the use of similarity transformations, the proposed nonlinear PDEs are transformed into a system of ODEs. The MATLAB software is utilized to construct the table and graphs which illustrate the numerical results. In-depth discussion is done by the effects of dimensionless factors on the velocity profile, temperature profile, skin fraction coefficient and local Nusselt number. Tables and graphs are used to present the results.

1.2 Plan of the Thesis

The information below gives a quick summary of the thesis contents. **Chapter 2** covers some fundamental definitions, dimentionless parameters, governing laws and the method which is used to obtained the numerical results of the flow problem.
Chapter 3 presents a review of "MHD radiative nanofluid flow in the porous medium caused by a nonlinear stretching sheet". Shooting technique is utilized to find the numerical outcomes of the governing flow equations.
Chapter 4 extends the work of [25] by adding the impact of inclined magnetic field with hybrid nanofluid. By utilizing similarity transformations we transform the set of governing nonlinear PDEs into the nonlinear ODEs. Results for various parameters are discussed through graphs and tables.
Chapter 5 gives the final remarks about the whole thesis.
References consulted for this thesis are listed in the **Biblography**.

Chapter 2

Preliminaries

This chapter covers some fundamental definitions, dimentionless parameters, governing laws and the method which are used to obtained the numerical results of the flow problem.

2.1 Some Basic Terminologies

In this section we will discuss about some basic definitions which are very helpful to understand the subsequent chapter.

Definition 2.1.1 (Fluid)

"A fluid is a substance that deforms continuously under the application of a shear (tangential) stress no matter how small the shear stress may be." [26]

Definition 2.1.2 (Fluid Mechanics)

"Fluid mechanics is that branch of science which deals with the behavior of the fluid (liquids or gases) at rest as well as in motion." [27]

Definition 2.1.3 (Fluid Dynamics)

"The study of fluid if the pressure forces are also considered for the fluids in motion, is called fluid dynamics." [28]

Definition 2.1.4 (Fluid Statics)

"The study of fluid at rest is called fluid statics." [27]

Definition 2.1.5 (Viscosity)

"Viscosity is defined as the property of a fluid which offers resistance to the movement of one layer of fluid over another adjacent layer of the fluid. Mathematically,

$$\mu = \frac{\tau}{\frac{\partial u}{\partial y}},$$

where μ is viscosity coefficient, τ is shear stress and $\frac{\partial u}{\partial y}$ represents the velocity gradient." [29]

Definition 2.1.6 (Kinematic Viscosity)

"It is defined as the ratio between the dynamic viscosity and density of fluid. It is denoted by symbol ν called **nu**. Mathematically,

$$\nu = \frac{\mu}{\rho}." \text{ [29]}$$

Definition 2.1.7 (Thermal Conductivity)

"The Fourier heat conduction law states that the heat flow is proportional to the temperature gradient. The coefficient of proportionality is a material parameter known as the thermal conductivity which may be a function of a number of variables." [30]

Definition 2.1.8 (Thermal Diffusivity)

"The rate at which heat diffuses by conducting through a material depends on the thermal diffusivity and can be defined as,

$$\alpha = \frac{k}{\rho C_p},$$

where α is the thermal diffusivity, k is the thermal conductivity, ρ is the density and C_p is the specifc heat at constant pressure." [31]

2.2 Types of Fluid

Fluid are divided into major two classes, one is Newtonian and other is non- Newtonian, which are explained in the following definitions.

Definition 2.2.1 (Ideal Fluid)

"A fluid, which is incompressible and has no viscosity, is known as an ideal fluid. Ideal fluid is only an imaginary fluid as all the fluids, which exist, have some viscosity." [27]

Definition 2.2.2 (Real Fluid)

"A fluid, which possesses viscosity, is known as a real fluid. In actual practice, all the fluids are real fluids." [29]

Definition 2.2.3 (Newtonian Fluid)

"A real fluid, in which the shear stress is directly proportional to the rate of shear strain (or velocity gradient) is known as a Newtonian fluid. Mathematically, it can be written as:

$$\tau_{xy} \propto \left(\frac{du}{dy}\right),$$
$$\tau_{xy} = \mu\left(\frac{du}{dy}\right),$$

where μ = Dynamic viscosity, τ_{xy} = Shear stress exerted by the fluid, and $\frac{du}{dy}$ = Velocity gradient perpendicular to the direction of the shear."

Water and alcohol are the common examples of Newtonian fluid. [29]

Definition 2.2.4 (Non-Newtonian Fluid)

"A real fluid in which the shear stress is not directly proportional to the rate of shear strain (or velocity gradient), is known as a non-Newtonian fluid. Mathematical, it can be expressed as:

$$\tau_{xy} \propto \left(\frac{du}{dy}\right)^m, \qquad m \neq 1$$
$$\tau_{xy} = k\left(\frac{du}{dy}\right)^m,$$

where k = Flow consistency coefficient, $\frac{du}{dy}$ = Shear rate, and n = Flow behaviour index."

Some examples of non-Newtonian fluids are toothpaste, shampoo, and honey etc. [29]

Definition 2.2.5 (Magnetohydrodynamics)

"Magnetohydrodynamics (MHD) is concerned with the mutual interaction of fluid flow and magnetic fields. The fluids in question must be electrically conducting and non-magnetic, which limits us to liquid metals, hot ionised gases (plasmas) and strong electrolytes." [32]

2.3 Types of Flow

To understand the true sense of any physical problem in fluid dynamics, we must be clear about what type of flow is considered in the physical model.

Definition 2.3.1 (Rotational Flow)

"Rotational flow is that type of flow in which the fluid particles while flowing along stream-lines, also rotate about their own axis." [27]

Definition 2.3.2 (Irrotational Flow)

"Irrotational flow is that type of flow in which the fluid particles while flowing along stream-lines, do not rotate about their own axis then this type of flow is called irrotational flow." [27]

Definition 2.3.3 (Compressible Flow)

"Compressible flow is that type of flow in which the density of the fluid changes from point to point or in other words the density (ρ) is not constant for the fluid, Mathematically,

$$\rho \neq k,$$

where k is constant." [29]

Definition 2.3.4 (Incompressible Flow)

"Incompressible flow is that type of flow in which the density is constant for the

fluid. Liquids are generally incompressible while gases are compressible, Mathematically,

$$\rho = k,$$

where k is constant." [27]

Definition 2.3.5 (Steady Flow)

"If the flow characteristics such as depth of flow, velocity of flow, rate of flow at any point in open channel flow do not change with respect to time, the flow is said to be steady flow. Mathematically,

$$\frac{\partial Q}{\partial t} = 0,$$

where Q is any fluid property." [29]

Definition 2.3.6 (Unsteady Flow)

"If at any point in open channel flow, the velocity of flow, depth of flow or rate of flow changes with respect to time, the flow is said to be unsteady. Mathematically,

$$\frac{\partial Q}{\partial t} \neq 0,$$

where Q is any fluid property." [29]

Definition 2.3.7 (Internal Flow)

"Flows completely bounded by a solid surfaces are called internal or duct flows." [33]

Definition 2.3.8 (External Flow)

"Flows over bodies immersed in an unbounded fluid are said to be an external flow." [33]

2.4 Modes of Heat Transfer

Heat transfer phenomena deals with laws of thermodynamics. To grasp the complete idea of the transfer we must be familiar with the modes of heat transfer.

Definition 2.4.1 (Heat Transfer)

"Heat transfer is a branch of engineering that deals with the transfer of thermal

energy from one point to another within a medium or from one medium to another due to the occurrence of a temperature difference." [34]

Definition 2.4.2 (Conduction)

"The transfer of heat within a medium due to a diffusion process is called conduction."

For example:

- Picking up a hot cup of tea and feeling heat,
- If a metal spoon is propped up in a pot of boiling water it will become hot,
- A radiator is a good example of conduction. [34]

Definition 2.4.3 (Convection)

"Convection heat transfer is usually defined as energy transport effected by the motion of a fluid. The convection heat transfer between two dissimilar media is governed by Newtons law of cooling."

For example:

If meat is still frozen when its time to start cooking, it will defrost more quickly when placed under running water than if it is immersed in water. The reason is the convection, or movement of the water and its heat circulation, will transfer heat more quickly into the frozen meat than if the meat sits immersed in water and has to absorb heat energy through conduction. [34]

Definition 2.4.4 (Thermal Radiation)

"Thermal radiation is defined as radiant (electromagnetic) energy emitted by a medium and is solely to the temperature of the medium."

For example:

- Electromagnetic radiation, such as radio waves, microwaves, infrared, visible light, ultraviolet, x-rays, and gamma radiation (γ).
- Particle radiation, such as alpha radiation (α), beta radiation (β), proton radiation and neutron radiation (particles of non-zero rest energy). [34]

2.5 Dimensionless Numbers

Dimentionless numbers are very useful numbers for describing the physical phenomenon of the problem. Following are some basic dimentionless numbers, which are necessary for our subsequent discussion.

Definition 2.5.1 (Prandtl Number)

"It is the ratio between the momentum diffusivity ν and thermal diffusivity α. Mathematically, it can be defined as

$$Pr = \frac{\nu}{\alpha} = \frac{\frac{\mu}{\rho}}{\frac{k}{C_p \rho}} = \frac{\mu C_p}{k},$$

where μ represents the dynamic viscosity, Cp denotes the specific heat and k stands for thermal conductivity. The relative thickness of thermal and momentum boundary layer is controlled by Prandtl number. This number expresses the ratio of the momentum diffusivity (viscosity) to the thermal diffusivity. It characterizes the physical properties of a fluid with convective and diffusive heat transfers." [33]

Definition 2.5.1 (Skin Friction Coefficient)

"It expresses the dynamic friction resistance originating in viscous fluid flow around a fixed wall. The skin friction coefficient can be defined as

$$C_f = \frac{2\tau_w}{\rho U_w^2},$$

where τ_w denotes the shear stress on the wall, ρ the density and U_w the free-stream velocity." [35]

Definition 2.5.3 (Eckert Number)

"It is the dimensionless number used in continuum mechanics. It describes the relation between flows and the boundary layer enthalpy difference and it is used to characterized heat dissipation. Mathematically,

$$Ec = \frac{u^2}{C_p \nabla T},$$

where C_p denotes the specific heat.∇T is differenc between wall temperature and local temperature" [33]

Definition 2.5.4 (Nusselt Number)

"It is the relationship between the convective to the conductive heat transfer through the boundary of the surface. It is a dimensionless number which was first introduced by the German mathematician Nusselt. Mathematically, it is defined as:

$$Nu = \frac{qL}{k},$$

where q stands for convective heat transfer, L stands for characteristics length and k stands for thermal conductivity." [35]

Definition 2.5.6 (Reynolds Number)

"It is defined as the ratio of inertia force of a flowing fluid and the viscous force of the fluid. Mathematically,

$$Re = \frac{VL}{\nu},$$

where V denotes the free stream velocity, L is the characteristic length and ν stands for kinematic viscosity." [29]

2.6 Governing Laws

In this section governing equations and fundamental laws are described which are important in the study of different flow problems.

Definition 2.6.1 (Conservation of Mass)

"The principle of conservation of mass can be stated as the time rate of change of mass in a fixed volume is equal to the net rate of flow of mass across the surface. The mathematical statement and the prescribe results in the following equation known as the continuity equation.

$$\frac{\partial \rho}{\partial t} + \nabla.(\rho \mathbf{v}) = 0,$$

where t is the time, ρ is the density of the medium, v the velocity vector, and ∇ is the nabla or del operator. If the fluid is an incompressible, the conservation of mass will be expressed by

$$\nabla.\mathbf{v} = 0.''$$

Definition 2.6.2 (Conservation of Momentum)

"The momentum equation states that the time rate of change of linear momentum of a given set of particles is equal to the vector sum of all the external forces acting on the particles of the set, provided Newtons third Law of action and reaction governs the internal forces. Mathematically, it can be written as:

$$\frac{\partial}{\partial t}(\rho\mathbf{u}) + \nabla.[(\rho\mathbf{u})\mathbf{u}] = \nabla.\mathbf{T} + \rho g."$$

Definition 2.6.3 (Energy Equation)

"The law of conservation of energy states that the time rate of change of the total energy is equal to the sum of the rate of work done by the applied forces and change of heat content per unit time.

$$\frac{\partial \rho}{\partial t} + \nabla.\rho\mathbf{u} = -\nabla.\mathbf{q} + Q + \phi,$$

where ϕ is the dissipation function." [34]

2.7 Shooting Technique

Shooting is a suitable numerical technique to solve the boundary value problem. To elaborate the shooting method, consider the following nonlinear boundary value problem.

$$\left.\begin{aligned} g''(x) &= g(x)g'(x) + 2g^2(x), \\ g(0) &= 0, \qquad g(G) = J. \end{aligned}\right\} \tag{2.1}$$

To reduce the order of the above boundary value problem, introduce the following notations.

$$g = S_1 \qquad g' = S_1' = S_2 \qquad g'' = S_2'. \tag{2.2}$$

As a result, (2.1) is converted into the following system of first order ODEs.

$$S_1' = S_2, \qquad S_1(0) = 0, \tag{2.3}$$

$$S_2' = S_1 S_2 + 2S_1^2, \qquad S_2(0) = t, \tag{2.4}$$

where t is an approximation for the missing starting condition.

The Runge-Kutta method of order four is used to numerically solve the aforementioned IVP. Choose the missing condition t in such a way that

$$S_1(G, t) = J. \tag{2.5}$$

For convenience, now onward $S_1(G, t)$ will be denoted by $S_1(t)$.
Let us further denote $S_1(t) - J$ by $H(t)$, so that

$$H(t) = 0. \tag{2.6}$$

The above equation can be solved by using Newton's method with the following iterative formula.

$$t^{n+1} = t^n - \frac{H(t^n)}{\frac{\partial H(t^n)}{\partial t}},$$

or

$$t^{n+1} = t^n - \frac{S_1(t^n) - J}{\frac{\partial S_1(t^n)}{\partial t}}. \tag{2.7}$$

To find $\frac{\partial S_1(t^n)}{\partial t}$, introduce the following notations.

$$\frac{\partial S_1}{\partial t} = S_3, \quad \frac{\partial S_2}{\partial t} = S_4. \tag{2.8}$$

The Newton's iterative method will acquire the following form as a result of these additional notations.

$$t^{n+1} = t^n - \frac{S_1(t) - J}{S_3(t)}. \tag{2.9}$$

To incorporate Newton's method, we include the following two equations in our system.

$$S_3' = S_4, \qquad S_3(0) = 0. \tag{2.10}$$

$$S_4' = S_3S_2 + S_1S_4 + 4S_1S_3, \qquad S_4(0) = 1. \tag{2.11}$$

Eventually the following initial value problem arises when all four ODEs, (2.3), (2.4), (2.10), and (2.11), are written together.

$$\begin{aligned} S_1' &= S_2, & S_1(0) &= 0. \\ S_2' &= S_1S_2 + 2S_1^2, & S_2(0) &= t. \\ S_3' &= S_4, & S_3(0) &= 0. \\ S_4' &= S_3S_2 + S_1S_4 + 4S_1S_3, & S_4(0) &= 1. \end{aligned}$$

Runge-Kutta method of order 4 will be used to numerically solve the combined system. This process will be repeated until the following criteria is met.

$$\mid S_1(t) - J \mid < \epsilon,$$

where "ϵ" is an arbitrary small positive number

Chapter 3

Nanofluid Flow over a Non-Linear Stretching Sheet

3.1 Introduction

This chapter provides a detailed review of the work presented by Jafar et al. [25]. The main focus is to study the numerical analysis of MHD nanofluid flow via a nonlinear stretching sheet saturated in a porous medium in the presence of a magnetic field, heat generation and thermal radiation. The controlling nonlinear PDEs are converted into a system of dimensionless ODEs using the similarity transformations. Using MATLAB, the shooting method is used to resolve ODEs. At the conclusion of this chapter, the numerical solution is used to describe the influence of various physical parameters over velocity and temperature profile. The generated numerical findings are examined using tables and graphs.

3.2 Mathematical Formulations of Model

A two dimentional MHD flow of nanofluid over a non-linear stretching sheet is considered under the effects of viscous dissipation, thermal radiation and heat generation. To the flow, Tiwari and Das model [6] is employed. Water is utilized

as base fluid and copper as nano particle. The variable stretching velocity, the variable magnetic field, and the variable permeability of the porous medium of the nanofluid flow are

$$U_w(x) = ax^n, \quad B(x) = B_0 x^{\frac{n-1}{2}}, \quad k(x) = k_0 x^{n-1},$$

where n is the stretching sheet parameter, a is the stretching constant, k_0 is the permeability constant and B_0 is the constant of magnetic field. The surface of the stretching sheet is also held at a temperature of $T_w = T_\infty + bx^{2n-1}$, where n is the parameter for surface temperature, b is a positive constant and T_∞ is the ambient temperature of the nanofluid. The geometry of the flow problem can be seen through Figure 3.1. The two dimentional model of the flow is given as: [25]

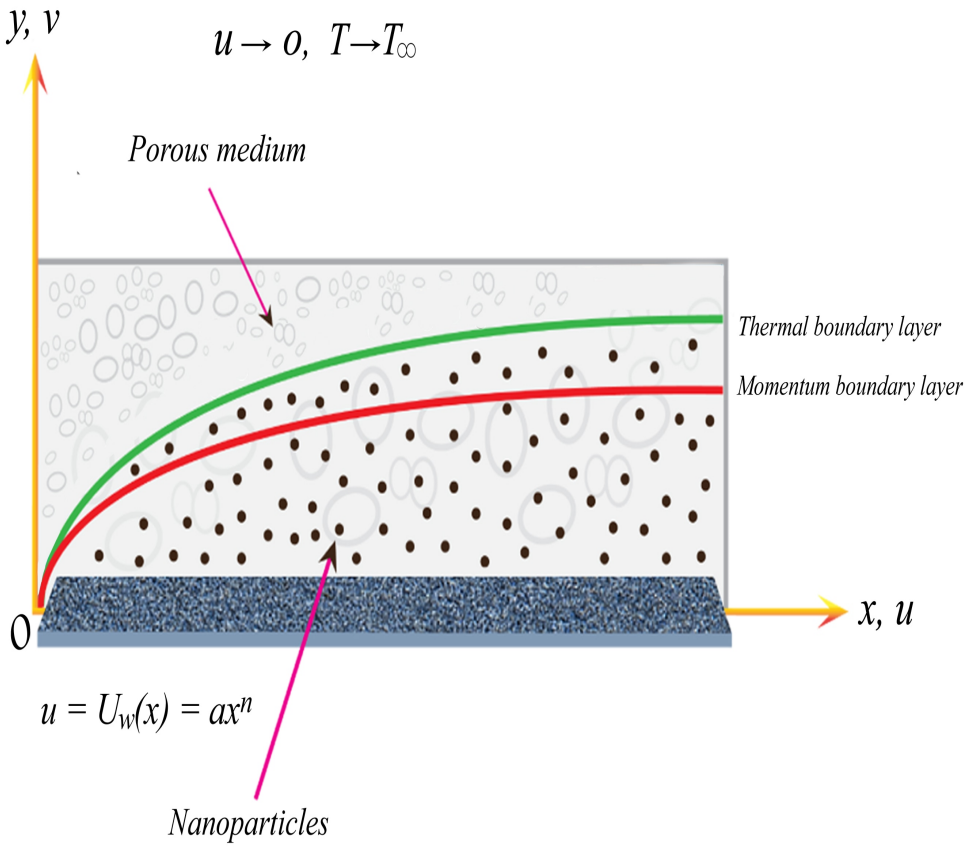

FIGURE 3.1: Systematic representation of physical model.

$$\frac{\partial u}{\partial x}+\frac{\partial v}{\partial y}=0, \tag{3.1}$$

$$\rho_{nf}\left(u\frac{\partial u}{\partial x}+v\frac{\partial u}{\partial y}\right)=\mu_{nf}\left(\frac{\partial^2 u}{\partial y^2}\right)-\frac{\mu_{nf}}{k(x)}u-\sigma_{nf}B^2(x)u, \tag{3.2}$$

$$u\frac{\partial T}{\partial x}+v\frac{\partial T}{\partial y}=\frac{\mu_{nf}}{(\rho C_p)_{nf}}\left(\frac{\partial u}{\partial y}\right)^2+\alpha_{nf}\left(\frac{\partial^2 T}{\partial y^2}\right)-\frac{1}{(\rho C_p)_{nf}}\left(\frac{\partial q_r}{\partial y}\right)+\frac{q}{(\rho C_p)_{nf}}(T-T_\infty). \tag{3.3}$$

where x denotes the direction of the sheet, y denotes the direction normal to the sheet, and u and v denote the horizontal and vertical velocities in the xy-plane, respectivly.

The corresponding boundary conditions have been taken as,

$$\left.\begin{aligned} &u=U_w(x)=ax^n, \quad v=0, \quad T=T_w=T_\infty+bx^{2n-1}, \quad at \quad y=0,\\ &u\to 0, \quad T\to T_\infty, \quad as \quad y\to\infty. \end{aligned}\right\} \tag{3.4}$$

ρ_{nf}, μ_{nf}, $(\rho C_p)_{nf}$, β_{nf}, σ_{nf}, $k(x)$, $\alpha_{nf}=\frac{k_{nf}}{(\rho C_p)_{nf}}$, k_{nf} and q are respectivly the effective density, coefficient of viscosity, heat capacitance at constant pressure, thermal expansion, electrical conductivity, variable permeability, thermal diffusivity, thermal conductivity of the nanofluids and heat generation constant respectivly. The radiative heat flux q_r is formulated as,

$$q_r=-\frac{4\sigma^*}{3k^*}\frac{\partial T^4}{\partial y}, \tag{3.5}$$

where k is the mean absorption coefficient and σ^* is the Stefan-Boltzman constant. The temperature T^4 can be expanded by the Taylor series about T_∞ as follows:

$$T^4=T_\infty^4+4T_\infty^3(T-T_\infty)+6T_\infty^2(T-T_\infty)^2+...$$

By ignoring the higher order terms, the T^4 can be expressed as,

$$T^4\approx T_\infty^4+4T_\infty^3(T-T_\infty),$$

$$T^4 \approx 4T_\infty^3 T - 3T_\infty^4.$$

The thermophysical characteristics of nanofluid are stated as follows: [6, 36, 37]:

$$\begin{aligned}
\alpha_{nf} &= \frac{k_f}{(\rho C_p)_{nf}}, \\
\rho_{nf} &= (1-\phi)\rho_f + \phi\rho_s, \\
\mu_{nf} &= \frac{\mu_f}{(1-\phi)^{2.5}}, \\
(\rho C_p)_{nf} &= (1-\phi)(\rho C_p)_f + \phi(\rho C_p)_s, \\
\frac{k_{nf}}{k_f} &= \frac{(k_s+2k_f)-2\phi(k_f-k_s)}{(k_s+2k_f)+\phi(k_f-k_s)}, \\
\frac{\sigma_{nf}}{\sigma_f} &= 1 + \frac{3\left(\frac{\sigma_s}{\sigma_f}-1\right)\phi}{\left(\frac{\sigma_s}{\sigma_f}+2\right)-\left(\frac{\sigma_s}{\sigma_f}-1\right)\phi},
\end{aligned}$$

where ϕ, ρ_f, ρ_s, μ_f, β_f, β_s, $(\rho C_P)_s$, σ_f, σ_s, k_f and k_s are respectivly the nanoparticles solid volume fraction, the density of the pure fluid, the density of the nanoparticles, the effective viscosity of the base fluid, the thermal expansion coefficient of the fluid, the thermal expansion coefficient of the nanoparticles, the heat capacitance of the fluid, the heat capacitance of the nanoparticles, the electrical conductivity of the fluid, the electrical conductivity of the nanoparticles, the thermal conductivity of the base fluid and the thermal conductivity of the solid friction.

3.3 Similarity Transformations

The following similarity transformations are employed to convert the mathematical model (3.1)-(3.3) into the system of ODEs. [25]

$$\left.\begin{aligned}
\psi(x,y) &= \sqrt{\frac{2\nu_f a}{n+1}}\, x^{\frac{n+1}{2}} f(\eta), \\
\eta &= y\sqrt{\frac{a(n+1)}{2\nu_f}}\, x^{\frac{n-1}{2}}, \\
\theta(\eta) &= \frac{T-T_\infty}{T_w-T_\infty},
\end{aligned}\right\} \tag{3.6}$$

where ψ stands for the stream function. The step-by-step process for converting (3.1)-(3.3) into the dimensionless form has been covered here. The conversion of continuity equation (3.1) is considered first. The following calculations will help us to show how continuity equation is satisfied. For this purpose, the follwoing derivatives are elaborated below.

$$u = \frac{\partial \psi}{\partial y}, \qquad v = -\frac{\partial \psi}{\partial x}.$$

From (3.6),

$$\begin{aligned}
u &= \frac{\partial}{\partial y}\left(\sqrt{\frac{2\nu a}{n+1}}x^{\frac{n+1}{2}}f(\eta)\right), \\
&= \sqrt{\frac{2\nu a}{n+1}}x^{\frac{n+1}{2}}f'(\eta)\frac{\partial \eta}{\partial y}, \\
&= \sqrt{\frac{2\nu a}{n+1}}x^{\frac{n+1}{2}}f'(\eta)\sqrt{\frac{a(n+1)}{2\nu}}x^{\frac{n-1}{2}}, \\
&= ax^n f'(\eta). \qquad (3.7) \\
v &= -\frac{\partial}{\partial x}\left(\sqrt{\frac{2a\nu}{n+1}}x^{\frac{n+1}{2}}f(\eta)\right), \\
&= -\left(\sqrt{\frac{2a\nu}{n+1}}\frac{\partial}{\partial x}x^{\frac{n+1}{2}}f(\eta) + \sqrt{\frac{2a\nu}{n+1}}x^{\frac{n+1}{2}}\frac{\partial}{\partial x}f(\eta)\right),
\end{aligned}$$

$$\begin{aligned}
&= -\left(\sqrt{\frac{2\nu a}{n+1}}\frac{n+1}{2}x^{\frac{n-1}{2}}f(\eta) + \sqrt{\frac{2\nu a}{n+1}}x^{\frac{n+1}{2}}f'(\eta)\frac{\partial \eta}{\partial x}\right) \\
&= -\sqrt{\frac{2\nu a}{n+1}}\left(\frac{n+1}{2}x^{\frac{n-1}{2}}f(\eta) + x^{\frac{n+1}{2}}f'(\eta)y\sqrt{\frac{a(n+1)}{2\nu}}\left(\frac{n-1}{2}\right)x^{\frac{n-3}{2}}\right), \\
&= -\sqrt{\frac{2\nu a}{n+1}}\left(\frac{n+1}{2}x^{\frac{n-1}{2}}f(\eta) + x^{\frac{n-1}{2}}\eta f'(\eta)\left(\frac{n-1}{2}\right)\right), \\
&= -\sqrt{\frac{2\nu a}{n+1}}x^{\frac{n-1}{2}}\frac{n+1}{2}\left(f(\eta) + \eta f'(\eta)\left(\frac{n-1}{n+1}\right)\right), \\
&= -\sqrt{\frac{\nu a(n+1)}{2}}x^{\frac{n-1}{2}}\left(f(\eta) - \eta f'(\xi)\left(\frac{n-1}{n+1}\right)\right), \\
&= -\sqrt{\frac{\nu a(n+1)}{2}}x^{\frac{n-1}{2}}\left(f(\eta) - \eta f'(\eta)\left(\frac{n-1}{n+1}\right)\right). \qquad (3.8)
\end{aligned}$$

Differentiating (3.7) w.r.t. x, we get

$$\begin{aligned}
\frac{\partial u}{\partial x} &= \frac{\partial}{\partial x}\left(af'(\eta)x^n\right),\\
&= a\frac{\partial}{\partial x}\left(f'(\eta)x^n\right),\\
&= a\left(nx^{n-1}f'(\eta) + x^n f''(\eta)\frac{\partial \eta}{\partial x}\right),\\
&= a\left(nx^{n-1}f'(\eta) + x^n f''(\eta) y\sqrt{\frac{a(n+1)}{2\nu_f}}\left(\frac{n-1}{2}\right)x^{\frac{n-3}{2}}\right),\\
&= a\left(nx^{n-1}f'(\eta) + x^n(\eta) f''(\eta)\sqrt{\frac{2\nu}{a(n+1)}}x^{\frac{1-n}{2}}\sqrt{\frac{a(n+1)}{2\nu}}\left(\frac{n-1}{2}\right)x^{\frac{n-3}{2}}\right),\\
&= ax^{n-1}\left(nf'(\eta) + \left(\frac{n-1}{2}\right)(\eta) f''(\eta)\right),\\
&= ax^{n-1}nf^{(}\eta) + ax^{n-1}\left(\frac{n-1}{2}\right)(\eta) f''(\eta). \qquad (3.9)
\end{aligned}$$

Diffirentiating (3.8) w.r.t. y, we get

$$\begin{aligned}
\frac{\partial v}{\partial y} &= \frac{\partial}{\partial y}\left[-\sqrt{\frac{(n+1)\nu a}{2}}x^{\frac{n-1}{2}}\left(f(\eta) + \eta f'(\eta)\left(\frac{n-1}{n+1}\right)\right)\right],\\
&= -\sqrt{\frac{(n+1)\nu a}{2}}x^{\frac{n-1}{2}}\left[\frac{\partial}{\partial y}f(\eta) + \left(\frac{n-1}{n+1}\right)\left(\frac{\partial}{\partial y}f'(\eta) + \eta\frac{\partial}{\partial y}f'(\eta)\right)\right],\\
&= -\sqrt{\frac{a(n+1)\nu}{2}}x^{\frac{n-1}{2}}\frac{\partial \eta}{\partial y}\left[f'(\eta) + \left(\frac{n-1}{n+1}\right)\left(f'(\eta) + \eta f''(\eta)\right)\right],\\
&= -\sqrt{\frac{a(n+1)\nu}{2}}x^{\frac{n-1}{2}}\sqrt{\frac{(n+1)a}{2\nu}}x^{\frac{n-1}{2}}\left[f'(\eta) + \left(\frac{n-1}{n+1}\right)\left(f'(\eta) + \eta f''(\eta)\right)\right],\\
&= -\frac{(n+1)a}{2}x^{n-1}\left[f'(\eta) + \left(\frac{n-1}{n+1}\right)\left(f'(\eta) + \eta f''(\eta)\right)\right],\\
&= -\frac{a}{2}x^{n-1}\left(\left(n+1\right)f'(\eta) + \left(n-1\right)\left(f' + \eta f''(\eta)\right)\right),\\
&= -\frac{a}{2}x^{n-1}2nf'(\eta) - \frac{a}{2}x^{n-1}(n-1)\eta f''(\eta),\\
&= -ax^{n-1}nf'(\eta) - ax^{n-1}\left(\frac{n-1}{2}\right)\eta f''(\eta). \qquad (3.10)
\end{aligned}$$

By using (3.9) and (3.10), we get

$$\Rightarrow \frac{\partial u}{\partial x} + \frac{\partial v}{\partial y} = ax^{n-1}nf'(\eta) + ax^{n-1}\frac{\binom{n-1}{}}{2}(\eta) f''(\eta) - ax^{n-1}nf'(\eta)$$

$$
\begin{aligned}
&- ax^{n-1}\left(\frac{n-1}{2}\right)\eta f''(\eta) = 0\\
&= 0. \qquad (3.11)
\end{aligned}
$$

The following calculations are useful to convert the momentum equation (3.2) into the dimentionless form.

$$
\begin{aligned}
& u = ax^n f'(\eta)\\
\Rightarrow & \frac{\partial u}{\partial y} = \frac{\partial}{\partial y}(ax^n f'(\eta)),\\
& = ax^n f''(\eta)\sqrt{\frac{a(n+1)}{2\nu}}x^{\frac{n-1}{2}}\\
& = ax^{\frac{3n-1}{2}}\sqrt{\frac{a(n+1)}{2\nu}}f''(\eta). \qquad (3.12)\\
\Rightarrow & \frac{\partial^2 u}{\partial^2 y} = \frac{\partial}{\partial y}\left(ax^{\frac{3n-1}{2}}\sqrt{\frac{a(n+1)}{2\nu}}f''(\eta)\right),\\
& = ax^{\frac{3n-1}{2}}\sqrt{\frac{a(n+1)}{2\nu}}\frac{\partial}{\partial y}f''(\eta),\\
& = ax^{\frac{3n-1}{2}}\sqrt{\frac{a(n+1)}{2\nu}}f'''(\eta)\frac{\partial \eta}{\partial y},\\
& = ax^{\frac{3n-1}{2}}\sqrt{\frac{a(n+1)}{2\nu}}f'''(\eta)\sqrt{\frac{a(n+1)}{2\nu}}x^{\frac{n-1}{2}},\\
& = a^2x^{2n-1}\left(\frac{n+1}{2\nu}\right)f'''(\eta),\\
\Rightarrow & \mu_{nf}\frac{\partial^2 u}{\partial^2 y} = \mu_{nf}a^2x^{2n-1}\left(\frac{n+1}{2\nu}\right)f'''(\eta).
\end{aligned}
$$

From (3.9), we know that

$$
\begin{aligned}
& \frac{\partial u}{\partial x} = anx^{n-1}f'(\eta) + ax^{n-1}\left(\frac{n-1}{2}\right)\eta f''(\eta).\\
\Rightarrow & u\frac{\partial u}{\partial x} = u\left(anx^{n-1}f'(\eta) + ax^{n-1}\left(\frac{n-1}{2}\right)\eta f''(\eta)\right)\\
& = a^2x^{2n-1}nf'(\eta) + a^2x^{2n-1}\left(\frac{n-1}{2}\right)\eta f'(\eta)f''(\eta).
\end{aligned}
$$

From equation (3.12), we know that

$$\begin{aligned}
\frac{\partial u}{\partial y} &= ax^{\frac{3n-1}{2}}\sqrt{\frac{a(n+1)}{2\nu}}f''(\eta).\\
\Rightarrow v\frac{\partial u}{\partial y} &= vax^{\frac{3n-1}{2}}\sqrt{\frac{a(n+1)}{2\nu}}f''(\eta),\\
&= -\sqrt{\frac{a\nu(n+1)}{2}}x^{\frac{n-1}{2}}\left(f(\eta)+\eta f'(\eta)\left(\frac{n-1}{n+1}\right)\right)\\
&\quad\left(ax^n f''(\eta)\sqrt{\frac{a(n+1)}{2}}x^{\frac{3n-1}{2}}\right),\\
&= -\sqrt{\frac{a\nu(n+1)}{2}}x^{\frac{n-1}{2}}\left(f(\eta)+\eta f'(\eta)\left(\frac{n-1}{n+1}\right)\right)\\
&\quad\left(ax^n f''(\eta)\sqrt{\frac{a(n+1)}{2}}x^{\frac{3n-1}{2}}\right),\\
&= -\sqrt{\frac{a\nu(n+1)}{2}}x^{\frac{n-1}{2}}f(\eta)ax^n f''(\eta)\sqrt{\frac{a(n+1)}{2\nu}}x^{\frac{3n-1}{2}},\\
&\quad -\sqrt{\frac{a\nu(n+1)}{2}}x^{\frac{3n-1}{2}}f'(\eta)(\eta)\left(\frac{n-1}{n+1}\right)ax^n f''(\eta)\sqrt{\frac{a(n+1)}{2\nu}}x^{\frac{3n-1}{2}},\\
&= -\frac{a^2(n+1)}{2}x^{2n-1}f(\eta)f''(\eta) - \frac{a^2(n+1)}{2}x^{2n-1}f'(\eta)f''(\eta)\eta\left(\frac{n-1}{n+1}\right).\\
\Rightarrow u\frac{\partial u}{\partial x} + v\frac{\partial u}{\partial y} &= a^2x^{2n-1}nf'^2(\eta) + a^2x^{2n-1}\left(\frac{n-1}{2}\right)\eta f'(\eta)f''(\eta)\\
&\quad -\frac{a^2(n+1)}{2}x^{2n-1}f(\eta)f''(\eta)\\
&\quad -\frac{a^2(n+1)}{2}x^{2n-1}f'(\eta)f''(\eta)\eta\left(\frac{n-1}{n+1}\right),\\
&= a^2x^{2n-1}nf'^2(\eta) - \frac{a^2(n+1)}{2}x^{2n-1}f(\eta)f''(\eta),\\
&= a^2x^{2n-1}nf'^2(\eta) - \frac{a^2(n+1)}{2}x^{2n-1}f(\eta)f''(\eta),\\
&= a^2x^{2n-1}\left(nf'^2(\eta) - \frac{(n+1)}{2}f(\eta)f''(\eta)\right).\\
\Rightarrow \rho_{nf}\left(u\frac{\partial u}{\partial x} + v\frac{\partial u}{\partial y}\right) &= \rho_{nf}a^2x^{2n-1}\left(nf'^2(\eta) - \frac{(n+1)}{2}f(\eta)f''(\eta)\right).\\
\Rightarrow \frac{u}{k(x)} &= \frac{\mu_n f}{k(x)}u = \frac{ax^n f'(\eta)}{k_0x^{1-n}} = \frac{ax^{2n-1}f'(\eta)}{k_0}\\
&= \mu_n f\frac{a^2x^{2n-1}f'(\eta)K}{\nu_f}. \qquad (3.13)\\
\Rightarrow \sigma_{nf}B^2(x)u &= \sigma_{nf}B_0^2x^{\frac{n-1}{2}}ax^n f'(\eta)\\
&= \sigma_{nf}ax^{2n-1}B_0^2f'(\eta). \qquad (3.14)
\end{aligned}$$

By using required values in (3.2), we get

$$\rho_{nf}a^2x^{2n-1}\left(nf'^2(\eta)-\frac{(n+1)}{2}f(\eta)f''(\eta)\right)=\mu_{nf}a^2x^{2n-1}\left(\frac{n+1}{2\nu}\right)f'''(\eta)$$
$$-\mu_n f\frac{a^2x^{2n-1}f'(\eta)K}{\nu_f}-\sigma_{nf}ax^{2n-1}B_0^2f'(\eta).$$
$$\Rightarrow \rho_{nf}a^2x^{2n-1}\left(\frac{n+1}{2}\right)\left[\left(\frac{2n}{n+1}\right)f'(\eta)-f(\eta)f''(\eta)\right]=\mu_{nf}a^2x^{2n-1}\left(\frac{n+1}{2\nu}\right)$$
$$\left[f'''(\eta)-\left(\frac{2\nu}{n+1}\right)\left(\frac{K}{\nu}+\frac{\sigma_{nf}}{\mu_{nf}}\frac{B_0^2}{a}\right)f'(\eta)\right].$$
$$\Rightarrow \nu\frac{\rho_{nf}}{\mu_{nf}}\left(\frac{n+1}{2}\right)\left[\left(\frac{2n}{n+1}\right)f'(\eta)-f(\eta)f''(\eta)\right]=f'''(\eta)-\left(\frac{2}{n+1}\right)$$
$$f'(\eta)\left[K+\nu\frac{\sigma_{nf}}{\mu_{nf}}\frac{B_0^2}{a}\right].$$
$$\Rightarrow -(1-\phi+\phi\frac{\rho_s}{\rho_f})(1-\phi)^{2.5}\left(f(\eta)f''(\eta)-\frac{2n}{n+1}\right)=f'''(\eta)-\left(\frac{2}{n+1}\right)f'(\eta)\Bigg[K$$
$$+M(1-\phi)^{2.5}\left(1+\frac{3\left(\frac{\sigma_s}{\sigma_f}-1\right)\phi}{\left(\frac{\sigma_s}{\sigma_f}+2\right)-\left(\frac{\sigma_s}{\sigma_f}-1\right)\phi}\right)\Bigg].$$

$$\Rightarrow f'''(\eta)+(1-\phi+\phi\frac{\rho_s}{\rho_f})(1-\phi)^{2.5}\left(f(\eta)f''(\eta)-\frac{2n}{n+1}\right)-\left(\frac{2}{n+1}\right)f'(\eta)\Bigg[K$$
$$+M(1-\phi)^{2.5}\left(1+\frac{3\left(\frac{\sigma_s}{\sigma_f}-1\right)\phi}{\left(\frac{\sigma_s}{\sigma_f}+2\right)-\left(\frac{\sigma_s}{\sigma_f}-1\right)\phi}\right)\Bigg]=0 \tag{3.15}$$

The derivation of some useful derivatives for the conversion of energy equation (3.3) into a dimentionless form is shown below:

$$\eta=\sqrt{\frac{a(n+1)}{2\nu}}yx^{\frac{n-1}{2}},\qquad \theta=\frac{T-T_\infty}{T_w-T_\infty},\qquad T=T_\infty+bx^{2n-1}\theta.$$
$$\Rightarrow \frac{\partial\eta}{\partial x}=\left(\frac{n-1}{2}\right)\left(\frac{\eta}{x}\right).$$
$$\Rightarrow \frac{\partial\eta}{\partial y}=\sqrt{\frac{a(n+1)}{2\nu}}x^{\frac{n-1}{2}}.$$
$$\Rightarrow \frac{\partial T}{\partial x}=b(2n-1)x^{2n-2}\theta+bx^{2n-1}\theta'\frac{\partial\eta}{\partial x}$$
$$=b(2n-1)x^{2n-2}\theta+bx^{2n-1}\theta'\left(\frac{n-1}{2}\right)\left(\frac{\eta}{x}\right).$$

$$\Rightarrow u\frac{\partial T}{\partial x} = ax^n f'\left(b(2n-1)x^{2n-2}\theta + bx^{2n-1}\theta'\left(\frac{n-1}{2}\right)\left(\frac{\eta}{x}\right)\right)$$
$$= ab(2n-1)x^{3n-1}f'(\eta)\theta + abx^{3n-1}\left(\frac{n-1}{2}\right)\eta\theta f'(\eta).$$
$$\Rightarrow \frac{\partial T}{\partial y} = bx^{2n-1}\theta'\frac{\partial \eta}{\partial y}$$
$$= bx^{2n-1}\theta'\sqrt{\frac{a(n+1)}{2\nu}}x^{\frac{n-1}{2}}.$$
$$\Rightarrow v\frac{\partial T}{\partial y} = -\sqrt{\frac{a\nu(n+1)}{2}}x^{\frac{n-1}{2}}\left(f(\eta) + \eta f'(\eta)\left(\frac{n-1}{n+1}\right)\right)$$
$$\left[bx^{2n-1}\theta'\sqrt{\frac{a(n+1)}{2\nu}}x^{\frac{n-1}{2}}\right]$$
$$= -abx^{3n-2}\frac{n+1}{2}\theta' - abx^{3n-2}\left(\frac{n-1}{2}\right)\eta\theta' f'(\eta).$$

By using all values, the left side of (3.3) will be:

$$u\frac{\partial T}{\partial x} + v\frac{\partial T}{\partial y} = ab(2n-1)x^{3n-2}f'(\eta)\theta + abx^{3n-2}\left(\frac{n-1}{2}\right)\eta\theta' f'(\eta)$$
$$- abx^{3n-2}\frac{n+1}{2}\theta' - abx^{3n-2}\left(\frac{n-1}{2}\right)\eta\theta' f'(\eta),$$
$$= abx^{3n-2}\left[2n-1f'(\eta)\theta - \frac{n+1}{2}\theta' f(\eta)\right].$$

$$\Rightarrow \frac{\partial^2 T}{\partial y^2} = bx^{2n-1}\sqrt{\frac{a(n+1)}{2\nu}}x^{\frac{n-1}{2}}\theta''\frac{\partial \eta}{\partial y}$$
$$= bx^{3n-2}\theta''\sqrt{\frac{a(n+1)}{2\nu}}\sqrt{\frac{a(n+1)}{2\nu}}$$
$$= \frac{ab(n+1)}{2\nu}x^{3n-2}\theta''.$$
$$\Rightarrow \alpha_{nf}\frac{\partial^2 T}{\partial y^2} = \alpha_{nf}\frac{ab(n+1)}{2\nu}x^{3n-2}\theta''.$$

Using (3.11),

$$\frac{\partial u}{\partial y} = ax^{\frac{3n-1}{2}}\sqrt{\frac{a(n+1)}{2\nu}}f''(\eta).$$
$$\Rightarrow \left(\frac{\partial u}{\partial y}\right)^2 = \left(ax^{\frac{3n-1}{2}}\sqrt{\frac{a(n+1)}{2\nu}}f''(\eta)\right)^2$$

$$= \frac{a^3(n+1)}{2\nu} f''^2 x^{3n-1}.$$

$$\Rightarrow \frac{\mu_{nf}}{(\rho Cp)_{nf}} \left(\frac{\partial u}{\partial y}\right)^2 = \frac{\mu_{nf}}{(\rho Cp)_{nf}} \frac{a^3(n+1)}{2\nu} f''^2(\eta) x^{3n-1}.$$

From (3.5),

$$q_r = -\frac{4\sigma*}{3k*}\frac{\partial T^4}{\partial y}.$$

$$\Rightarrow \frac{\partial q_r}{\partial y} = -\frac{\partial}{\partial y}\left(\frac{4\sigma*}{3k*}\left(\frac{\partial}{\partial y}\left(4T_\infty^3 T - 3T_\infty^4\right)\right)\right),$$

$$= -\frac{16\sigma*}{3k*} T_\infty^3 \frac{\partial^2 T}{\partial y^2},$$

$$= -\frac{16\sigma*}{3k*} T_\infty^3 \frac{ab(n+1)}{2\nu} x^{3n-2}\theta''.$$

$$\Rightarrow \frac{1}{(\rho Cp)_{nf}}\frac{\partial q_r}{\partial y} = \frac{1}{(\rho Cp)_{nf}} \frac{16\sigma*}{3k*} T_\infty^3 \frac{ab(n+1)}{2\nu} x^{3n-2}\theta''.$$

By using all values in (3.3), we get

$$abx^{3n-2}\left[2n-1 f'(\eta)\theta - \frac{n+1}{2}\theta' f(\eta)\right] = \alpha_{nf}\frac{ab(n+1)}{2\nu}x^{3n-2}\theta''$$
$$+ \frac{\mu_{nf}}{(\rho Cp)_{nf}}\frac{a^3(n+1)}{2\nu} f''^2(\eta) x^{3n-1}$$
$$- \frac{1}{(\rho Cp)_{nf}}\frac{16\sigma*}{3k*}T_\infty^3\frac{ab(n+1)}{2\nu}x^{3n-2}\theta'' - \frac{q}{(\rho Cp)_{nf}}(T - T_\infty)$$
$$\Rightarrow (2n-1)f'(\eta)\theta - \frac{n+1}{2}\theta' f(\eta) = \frac{k_n f}{(\rho Cp)_{nf}}\frac{n+1}{2v}\theta''$$
$$- \frac{1}{(\rho Cp)_{nf}}\frac{16\sigma*}{3k*}T_\infty^3\frac{(n+1)x}{2\nu}\theta'' + \frac{\mu_{nf}}{(\rho Cp)_{nf}}\frac{a^3(n+1)x}{2\nu b} f''^2(\eta) - q(\rho Cp)_{nf}x^{1-n}\theta.$$
$$\Rightarrow \theta'' + \frac{16\sigma*}{k_{nf}3k*}T_\infty^3\theta'' + \frac{\mu_{nf}a^2}{k_{nf}b}xf'' - \frac{2(2n-1)}{n+1}\frac{(\rho Cp)_{nf}}{k_{nf}}\nu f'\theta$$
$$+ \frac{(\rho Cp)_{nf}}{k_{nf}}\nu f'\theta + \frac{2q\nu x^{1-n}}{k_{nf}a(n+1)}\theta = 0.$$
$$\Rightarrow \theta'' + \frac{4R}{3}\theta'' + \frac{\mu_{nf}a^2 x}{k_{nf}b}f'' - \frac{2(2n-1)}{n+1}\frac{(\rho Cp)_{nf}}{k_{nf}}\nu f'\theta + \frac{(\rho Cp)_{nf}}{k_{nf}}\nu f'\theta$$
$$+ \frac{2q\nu x^{1-n}}{k_{nf}a(n+1)}\theta = 0.$$
$$\Rightarrow \theta''\left(1 + \frac{4R}{3}\right) + \frac{\nu\rho a^2 x}{k_{nf}b(1-\phi)^{2.5}}(f'')^2 + \left(f\theta' - \frac{2(2n-1)}{n+1}f'\theta\right)$$
$$\frac{\nu}{\alpha}\frac{\alpha(\rho Cp)_{nf}}{k_{nf}} + \frac{2}{n+1}\frac{qx}{k_{nf}(\rho Cp)_f}\nu(\rho Cp)_f\theta = 0.$$

$$
\begin{aligned}
&\Rightarrow \theta''\left(1+\frac{4R}{3}\right)+\frac{k}{k_{nf}}\frac{\nu}{\alpha}\frac{a^2x^{2n-1}}{(\rho Cp)_f b(1-\phi)^{2.5}x^{2n-1}}(f'')^2\frac{k}{k_{nf}}\Bigg(f\theta'\\
&\quad-\left(\frac{2(2n-1)}{n+1}\right)f'\theta\Bigg)\frac{\nu}{\alpha}\frac{(\rho Cp)_{nf}}{(\rho Cp)_f}\\
&\quad+\frac{k}{k_{nf}}\left(\frac{2}{n+1}\right)\frac{qx}{(\rho Cp)_f a x^n}\frac{\nu}{\alpha}\theta=0.\\
&\Rightarrow \theta''\left(1+\frac{4R}{3}\right)+\frac{k_f}{k_{nf}}P_r\left(\frac{E_c}{(1-\phi)^{2.5}}\right)(f'')^2+\frac{k_f}{k_{nf}}\Bigg(f\theta'\\
&\quad-\left(\frac{2(2n-1)}{n+1}\right)f'\theta\Bigg)P_r\left(1-\phi+\phi\left(\frac{(\rho Cp)_s}{(\rho Cp)_f}\right)\right)\\
&\quad+\frac{k_f}{k_{nf}}\left(\frac{2}{n+1}\right)Q\theta=0.\\
&\Rightarrow \frac{k_{nf}}{k_f}\left(1+\frac{4R}{3}\right)\theta''+P_r\left(\frac{E_c}{(1-\phi)^{2.5}}\right)(f'')^2\Bigg(f\theta'\\
&\quad-\left(\frac{2(2n-1)}{n+1}\right)f'\theta\Bigg)P_r\left(1-\phi+\phi\left(\frac{(\rho Cp)_s}{(\rho Cp)_f}\right)\right)\\
&\quad+\left(\frac{2}{n+1}\right)Q\theta=0. \qquad (3.16)
\end{aligned}
$$

To transform the relevant BCs into their non-dimensional form, the following calculations are implemented:

$$
\begin{aligned}
&u=U_w(x)=ax^n, && at \quad y=0.\\
\Rightarrow\quad &u=af'(\eta)x^n.\\
\Rightarrow\quad &af'(\eta)=ax^n,\\
\Rightarrow\quad &f'(\eta)=1, && at \quad \xi=0.\\
\Rightarrow\quad &f'(0)=1.\\
&v=0, && at \quad y=0.\\
\Rightarrow\quad &-x^{\frac{n-1}{2}}\sqrt{\frac{2\nu_f a}{n+1}}\left(\frac{n+1}{2}\right)f(\eta)-ax^{n-1}y\left(\frac{n-1}{2}\right)f'(\eta)=0,\\
& && at \quad \eta=0.\\
\Rightarrow\quad &-x^{\frac{n-1}{2}}\sqrt{\frac{a\nu_f(n+1)}{2}}f(0)=0, && at \quad \eta=0.\\
\Rightarrow\quad &f(0)=0.
\end{aligned}
$$

$$
\begin{aligned}
& T = T_w, && at \quad y = 0. \\
\Rightarrow \quad & \theta(\eta)(T_w - T_\infty) + T_\infty = T_w, \\
\Rightarrow \quad & \theta(\eta)(T_w - T_\infty) = (T_w - T_\infty), \\
\Rightarrow \quad & \theta(\eta) = 1, && at \quad \eta = 0. \\
\Rightarrow \quad & \theta(0) = 1. \\
& u \to (0), && as \quad y \to \infty. \\
\Rightarrow \quad & af'(\eta)x^n \to (0), \\
\Rightarrow \quad & ax^n f'(v) \to (0), \\
\Rightarrow \quad & f'(\eta) \to (0), && as \quad \eta \to \infty. \\
\Rightarrow \quad & f'(\infty) \to 0. \\
& T \to T_\infty, && as \quad y \to \infty. \\
\Rightarrow \quad & \theta(\eta)(T_w - T_\infty) + T_\infty \to T_\infty, \\
\Rightarrow \quad & \theta(\eta)(T_w - T_\infty) \to 0, && as \quad \eta \to \infty. \\
\Rightarrow \quad & \theta(\eta) \to 0, && as \quad \eta \to \infty. \\
\Rightarrow \quad & \theta(\infty) \to 0.
\end{aligned}
$$

The final dimensionless form of the governing model is

$$
\begin{aligned}
& f'''(\eta) + (1 - \phi + \phi\frac{\rho_s}{\rho_f})(1 - \phi)^{2.5}\left(f(\eta)f''(\eta) - \frac{2n}{n+1}\right) - \left(\frac{2}{n+1}\right)f'(\eta) \\
& \left[K + M(1-\phi)^{2.5}\left(1 + \frac{3\left(\frac{\sigma_s}{\sigma_f} - 1\right)\phi}{\left(\frac{\sigma_s}{\sigma_f} + 2\right) - \left(\frac{\sigma_s}{\sigma_f} - 1\right)\phi}\right)\right] = 0, \qquad (3.17) \\
& \frac{k_{nf}}{k_f}\left(1 + \frac{4R}{3}\right)\theta'' + P_r\left(\frac{E_c}{(1-\phi)^{2.5}}\right)(f'')^2\left(f\theta' - \left(\frac{2(2n-1)}{n+1}\right)f'\theta\right) \\
& P_r\left(1 - \phi + \phi\left(\frac{(\rho Cp)_s}{(\rho Cp)_f}\right)\right) + \left(\frac{2}{n+1}\right)Q\theta = 0. \qquad (3.18)
\end{aligned}
$$

The corresponding BCs in the dimensionless form are gievn below:

$$
\left.
\begin{aligned}
& f(0) = 0, \quad f'(0) = 1, \quad \theta(0) = 1. \\
& f'(\infty) \to 0, \quad \theta(\infty) \to 0.
\end{aligned}
\right\} \qquad (3.19)
$$

The primes denotes the derivatives of the function f with respect to η, ϕ is the nanoparticle volume fraction, n is the non-linear stretching parameter, M is the magnetic parameter, K is the permeability parameter, R is the radiation parameter, Pr is the Prandtl number, Ec is the Eckert number, and Q is the heat generation parameter which are formulated as:

$$\left.\begin{aligned} M &= \frac{\sigma_f B_0^2}{\rho_f a x^{-1}}, \qquad & K &= \frac{\nu_f}{a k_0}, \\ R &= \frac{4\sigma^* T_\infty^3}{k_{nf} k^*}, \qquad & Pr &= \frac{\nu_f}{\alpha_f}, \\ Ec &= \frac{U_w^2}{(c_p)_f (T_w - T_\infty)}, \quad & Q &= \frac{qx}{(\rho c_p)_f U_w}. \end{aligned}\right\}$$

To find the dimentionless form of skin friction coefficient the following calculation are considered.

$$\begin{aligned} C_f &= \frac{\tau_w|_{y=0}}{\rho_f U_w^2(x)}, \\ \tau_w &= \mu_{nf}\left(\frac{\partial u}{\partial y}\right)_{y=0}. \end{aligned} \tag{3.20}$$

where,

$$\begin{aligned} \frac{\partial u}{\partial y} &= a x^n f''(\eta)\sqrt{\frac{a(n+1)}{2\nu}} x^{\frac{n-1}{2}}. \\ \frac{\partial u}{\partial y} &= a x^n f''(\eta)\sqrt{\frac{a(n+1)}{2\nu}} x^{\frac{n-1}{2}}. \\ \Rightarrow C_f &= \frac{\mu_{nf}}{\rho_f u_w^2} a x^n f''(\eta)\sqrt{\frac{a(n+1)}{2\nu}} x^{\frac{n-1}{2}}, \\ &= \frac{\mu_f}{\rho_f u_w^2 (1-\phi)^{2.5}} a x^{\frac{3n-1}{2}} f''(\eta)\sqrt{\frac{a(n+1)}{2\nu}}, \\ &= \frac{\rho_f \nu}{\rho_f a^2 x^{2n}(1-\phi)^{2.5}} a x^{\frac{3n-1}{2}} f''(\eta)\sqrt{\frac{a(n+1)}{2\nu}}, \\ &= \frac{v^{\frac{1}{2}}}{(1-\phi)^{2.5} a^{\frac{1}{2}} x^{\frac{n+1}{2}}} f''(\eta)\sqrt{\frac{(n+1)}{2}}, \\ &= \frac{1}{(1-\phi)^{2.5} Re_x^{\frac{1}{2}}} f''(\eta)\left(\frac{n+1}{2}\right), \\ \Rightarrow C_f Re_x^{\frac{1}{2}} &= \frac{1}{(1-\phi)^{2.5}} f''(\eta)\left(\frac{n+1}{2}\right). \end{aligned}$$

Here Re_x is the Reynolds number which is formulated as follows:

$$Re = \frac{a}{\nu} x^{\frac{n+1}{2}}.$$

The dimentional form of the local Nusselt number is formulated as follows,

$$Nu_x = \frac{x q_w}{k_f (T_w - T_\infty)}, \tag{3.21}$$

where

$$q_w = \left(- \left(k_{nf} + \frac{16\sigma^* T_\infty^3}{3k^*} \right) \left(\frac{\partial T}{\partial y} \right) \right)_{y=0}$$

As computed earlier,

$$\frac{\partial T}{\partial y} = (T_w - T_\infty)\, \theta'(\eta) \sqrt{\frac{a(n+1)}{2\nu}} x^{\frac{n-1}{2}}$$

$$\begin{aligned}
\Rightarrow Nu_x &= - \frac{x \left(k_{nf} + \frac{16\sigma^* T_\infty^3}{3k^*} \right) \left(\frac{\partial T}{\partial y} \right)_{y=0}}{k_f (T_w - T_\infty)}, \\
&= - \frac{x \left(k_{nf} + \frac{16\sigma^* T_\infty^3}{3k^*} \right)}{k_f (T_w - T_\infty)} (T_w - T_\infty)\, \theta'(\eta) \sqrt{\frac{a(n+1)}{2\nu}} x^{\frac{n-1}{2}}, \\
&= - \frac{k_{nf}}{k_f} \left(1 + \frac{4}{3} R \right) x^{\frac{n+1}{2}} \theta' \left(\frac{a(n+1)}{2\nu} \right)^{\frac{1}{2}}, \\
&= - \frac{k_{nf}}{k_f} \left(1 + \frac{4}{3} R \right) \theta' \left(\frac{n+1}{2} \right)^{\frac{1}{2}} \left(\frac{a x^{n+1}}{2\nu} \right)^{\frac{1}{2}}, \\
&= - \frac{k_{nf}}{k_f} \left(1 + \frac{4}{3} R \right) \sqrt{\frac{n+1}{2}} \theta'(\eta) Re_x^{\frac{1}{2}}, \\
\Rightarrow Re_x^{\frac{-1}{2}} Nu_x &= - \frac{k_{nf}}{k_f} \left(1 + \frac{4}{3} R \right) \left(\frac{n+1}{2} \right)^{\frac{1}{2}} \theta'(\eta).
\end{aligned}$$

3.4 Solution Methodology

One can observe that (3.15) is independent of θ ,so it can be solved first. The ordinary differential equation (3.15) is solved using the shooting technique. The notations listed below have been considered in order to transform the momentum

equation into the system of first order ODEs.

$$f = Y_1, \qquad f' = Y_1' = Y_2, \qquad f'' = Y_1'' = Y_2' = Y_3, \qquad f''' = Y_3'.$$

$$\begin{aligned}
&Y_1' = Y_2, && Y_1(0) = 0.\\
&Y_2' = Y_3, && Y_2(0) = 1.\\
&Y_3' = -(1-\phi+\phi\frac{\rho_s}{\rho_f})(1-\phi)^{2.5}\left(Y_1Y_3 - \frac{2n}{n+1}Y_2^2\right)\\
&\quad -\left(\frac{2}{n+1}\right)Y_2\Bigg[K + M(1-\phi)^{2.5}\\
&\quad \left(1+\frac{3\left(\frac{\sigma_s}{\sigma_f}-1\right)\phi}{\left(\frac{\sigma_s}{\sigma_f}+2\right)-\left(\frac{\sigma_s}{\sigma_f}-1\right)\phi}\right)\Bigg], && Y_3(0) = s.
\end{aligned}$$

The aforementioned IVP will be solved by Runge-Kutta method of order four using numbers. Furthermore, the missing condition s is selected in such a way that the following condition must hold:

$$Y_2(\eta_\infty, s) = 0.$$

The Newton's method will be used to determine s. This approach has the following iterative structure which is used to find the value of the missing condition s in a systematic manner.

$$s^{n+1} = s^n - \frac{Y_2(\eta_\infty, s)}{\frac{\partial}{\partial s}Y_2(\eta_\infty, s)}$$

Let us introduce new notations which will be fruitful to develop a complete first order initial value problem that will be solved using shooting technique.

$$\frac{\partial Y_1}{\partial s} = Y_4, \qquad \frac{\partial Y_2}{\partial s} = Y_5, \qquad \frac{\partial Y_3}{\partial s} = Y_6.$$

These new notations lead to a change in the shape of Newton's iterative scheme as follows:

$$s^{n+1} = s^n - \frac{Y_2(\eta_\infty, s)}{Y_5(\eta_\infty, s)}.$$

By differentiating the system of three first order ODEs with respect to the missing condition s, we now obtain another system of ODEs.

$$
\begin{aligned}
Y_4' &= Y_5, && Y_4(0) = 0.\\
Y_5' &= Y_6, && Y_5(0) = 0.\\
Y_6' &= -(1-\phi+\phi\frac{\rho_s}{\rho_f})(1-\phi)^{2.5}\left(Y_1 y6 - \frac{2n}{n+1}\right)2Y_2Y_5\\
&\quad -\left(\frac{2}{n+1}\right)Y_5\Bigg[K + M(1-\phi)^{2.5}\\
&\quad \left(1+\frac{3\left(\frac{\sigma_s}{\sigma_f}-1\right)\phi}{\left(\frac{\sigma_s}{\sigma_f}+2\right)-\left(\frac{\sigma_s}{\sigma_f}-1\right)\phi}\right)\Bigg], && Y_6(0) = 1.
\end{aligned}
$$

The following expression is the stoping criteria of Newton's method,

$$| Y_2(\xi_\infty, s) | < \epsilon,$$

where $\epsilon > 0$ is an arbitrarily small positive number. From now onward ϵ has been taken as 10^{-10}.

The shooting method will be used to numerically solve the equation (3.16), by assuming that f is a known function.

Let us consider the following notations.

$$\theta = Z_1, \quad \theta' = Z_1' = Z_2, \quad \theta'' = Z_2'.$$

Consequently, the energy equation (3.16) is transformed into the system of first order ODEs shown below.

$$
\begin{aligned}
Z_1' &= Z_2, && Z_1(0) = 1.\\
Z_2' &= \frac{k_f}{k_{nf}\left(1+\frac{4}{5}R\right)}\Bigg[-P_r\left(\frac{E_c}{(1-\phi)^{2.5}}\right)(f'')^2\\
&\quad -\left(f\theta' - \left(\frac{2(2n-1)}{n+1}\right)f'Z_2\right)\\
&\quad P_r\left(1-\phi+\phi\left(\frac{(\rho Cp)_s}{(\rho Cp)_f}\right)\right) - \left(\frac{2}{n+1}\right)QZ_1\Bigg], && z_2(0) = t.
\end{aligned}
$$

The Runge-Kutta method of order four is used to numerically solve the aforementioned initial value problem (IVP). The missing condition t in the aforementioned initial value problem must meet the following relation.

$$Z_1(\eta_\infty, t) = 0.$$

The Newton's iterative formula given below will be used to solve the equation,

$$t^{n+1} = t^n - \frac{Y_1(\eta_\infty, t)}{Y_1'(\eta_\infty, t}.$$

Let us consider the following notations,

$$\frac{\partial Z_1}{\partial t} = Z_3 \qquad\qquad \frac{\partial Z_2}{\partial Z} = Z_4. \tag{3.22}$$

We now obtain a separate system of ODEs by differentiating the system of two first order ODEs with regard to t.

$$\begin{aligned}
Z_3' &= Z_4, && Z_3(0) = 0.\\
Z_4' &= -\frac{k_f}{k_{nf}\left(1+\frac{4}{5}R\right)}\Bigg[- P_r\left(\frac{E_c}{(1-\phi)^{2.5}}\right)(f'')^2 \\
&\quad - \left(f\theta' - \left(\frac{2(2n-1)}{n+1}\right) f' Z_2\right) \\
&\quad P_r\left(1-\phi+\phi\left(\frac{(\rho Cp)_s}{(\rho Cp)_f}\right)\right) - \left(\frac{2}{n+1}\right) Q Z_1\Bigg], && Z_4(0) = 1.
\end{aligned}$$

The stoping condition of shooting method is defined as

$$\mid Z_1(\eta_\infty, t) \mid < 10^{-10}.$$

3.5 Representation of Tables and Graphs

In this section, the numerical findings for the momentum and energy equation are discussed using tables and graphs. The numerical information displayed in the tables and graphs is actually based on the variation of different dimentionless

parameters employed in the ODEs. The effect of dimensionless parameters on the skin friction coefficient and local Nusselt number has been thoroughly discussed in Table 3.1 and 3.2. At the end of this section, graphical visualization of the impact of various dimentionless parameters on velocity and temperature profile is explained in detail.

3.5.1 Skin Friction Coefficient

Table 3.1 shows the effect of the nonlinear stretching parameter, magnetic parameter, nanoparticle volume fraction, and permeability parameter on the skin friction coefficient. The following findings have been noted.

- With rising values of the magnetics parameter, the skin friction coefficient drops.
- The skin friction coefficient decreases with an increasing values of the nanoparticle volume fraction.
- Due to the rising values of permeability parameter, the skin friction coefficient falls.
- The skin friction coefficient decreases as the nonlinear stretching parameter's values increase.

Table 3.1 includes the interval I_f for initial guesses that direct us toward a convergent numerical solution.

TABLE 3.1: Numerical results of $(Re_x)^{\frac{1}{2}}C_f$ for different parameters

M	ϕ	K	n	$(Re_x)^{\frac{1}{2}}C_f$	I_f
2.0	0.1	0.25	2.0	-2.701788	[-1.0, 1]
2.2				-2.749483	[-0.5, 1]
2.4				-2.796382	[-0.5, 1]
2.6				-2.842521	[-1.0, 1]
	0.2			-3.540462	[-0.5, 1]
	0.3			-4.635428	[-1.0, 1]
	0.4			-6.157362	[-0.5, 1]
		0.35		-2.732914	[-0.5, 1]
		0.45		-2.763698	[-1.0, 1]
		0.55		-2.794150	[-1.0, 1]
			2.1	-2.737339	[-1.0, 1]
			2.2	-2.772433	[-1.0, 1]
			2.3	-2.807088	[-1.0, 1]

3.5.2 Local Nusselt Number

The impact of different dimentionless parameters on the local Nusselt number is thoroughly discussed in Table 3.2. The following observation have been made from table.

- The Nusselt number shows a decreasing behaviour due to an increasing Eckert number.
- As radiation parameter values grow, the Nusselt number rapidly increases.
- The Nusselt number exhibits a quick increase as a result of rising non linear stretching parameter.
- Due to an increase in the values of magnetic parameter, the Nusselt number decreases.

- The Nusselt number shows decreasinf pattern due to an increase in Prondtl number.
- An increase in heat generation parameter results a sudden decrease in Nusselt number.

The I_θ in Table 3.2 is the interval for initial guesses that direct us toward a convergent numerical solution.

TABLE 3.2: Results of $-(Re_x)^{\frac{-1}{2}}Nu_x$ when $\phi = 0.5$ and $K = 1.0$

Ec	R	n	M	Pr	Q	$-(Re_x)^{\frac{-1}{2}}Nu_x$	I_θ
0.2	0.5	2.0	2.0	6.2	0.1	0.652650	[-0.9,1.0]
0.3						-0.860422	[-0.9,1.0]
0.4						-2.373495	[-0.9,1.0]
0.5						-3.886568	[-0.9,1.0]
	0.6					0.713863	[-0.9,1.0]
	0.7					0.773891	[-0.9,1.0]
	0.8					0.832802	[-0.9,1.0]
		2.5				1.190183	[-0.9,1.0]
		3.0				1.638368	[-0.9,1.0]
		3.5				2.026851	[-0.9,1.0]
			2.5			0.585093	[-1.0,1.0]
			3.0			0.517789	[-1.0,1.0]
			3.5			0.450743	[-1.0,1.0]
				5.0		0.671614	[-1.0,1.0]
				5.5		0.664855	[-0.9,1.0]
				6.0		0.656423	[-1.0,1.0]
					0.3	0.392177	[-0.8,0.9]
					0.5	0.101935	[-1.0,1.0]
					0.7	-0.228809	[-1.0,0.8]

3.5.3 Velocity and Temperature Profiles

The behaviour of the velocity and temperature profile for different values of the nanoparticle volume fraction ϕ with and without the magnetic field M is shown in Figures 3.2, 3.3, 3.4, and 3.5. Increase in ϕ causes increase in horizontal velocity and the thickness of the momentum boundary layer also increases. Similar to this, the temperature profile is boosted as the volume percentage of nanoparticles is increased.This is caused by the fact that when more solid particles are suspended in the base fluid, the thermal conductivity of the fluid increases by increasing the heat transmission. The thickness of the thermal boundary layer also increases as a result of the change in temperature profile. Additionally, it can be seen from these figures that, for the same values of ϕ, the effect of the magnetic field on the nanoparticle volume fraction is greater when compared the temperature profile with velocity profile.

The impact of the permeability parameter K on the velocity field and temperature distribution is shown in Figures 3.6 and 3.7. An increase in K reduces the thickness of the momentum boundary layer by strength the porous layer, and K also improves the temperature distribution in the boundary layer region. Physically, Darcians body force is moving the heat from the solid wall to the flow region.

The effect of the nonlinear stretching sheet parameter n on the velocity and temperature profile is depicted in Figures 3.8 and 3.10.The velocity profile is increased as n is increased and the momentum boundary layer thickens. In contrast, a rise in n causes a reduction in the temperature profile, which causes the heat transfer to increase.

The variation of several values of the heat generation parameter Q on the temperature profile is shown in Figure 3.11. The thermal boundary layer produces heat whenever Q rises in a positive direction. This process thickens the thermal boundary layer, which suggests that heat energy is released and thus raises the temperature of the fluids.

Figure 3.12 shows that the temperature profile increases as the Eckert number increases. High Eckert number in nanofluids generates thermal energy more quickly and intensely, which enhances the temperature distribution and, as a result, thickens the thermal layer. This is because nanofluids is viscosity absorbs heat energy from the flow which intansly the heat energy by frictional heating and transforms it into internal energy, which then heats the nanofluid thermal energy gain.
The temperature distribution is affected by thermal radiation, as seen in Figure 3.13. It has been noted that the temperature distribution widens as the thermal radiation parameter R rises. The fluid releases heat energy from the flow region in response to an increase in the radiation parameter, which raises the temperature of the nanofluid and cools the system as a result. When the radiation parameter has a high value, the system produces more heat, which eventually raises the fluid's temperature and lengthens the thermal boundary layer.

Figures 3.14 and 3.15 illustrate that how the magnetic parameter M affects the velocity and temperature. Unexpectedly, a larger magnetic force increases the resistance to nanofluid flow. The thickness of the momentum boundary layer decreased due to this reduction in velocity profile, however the thickness of the thermal boundary layer increased, due to the Lorentz force created by the higher values of M.

The effect of the Prandtl number on the temperature profile is depicted in Figure 3.9. The graph demonstrates that when the values of Pr rise, the temperature profile is dropping. The graph clearly shows that an increase in Pr causes the temperature distribution to decrease and reduced the thickness of the thermal boundary layer. This suggests that the heat will spread quickly with higher values of prandtl parameter.

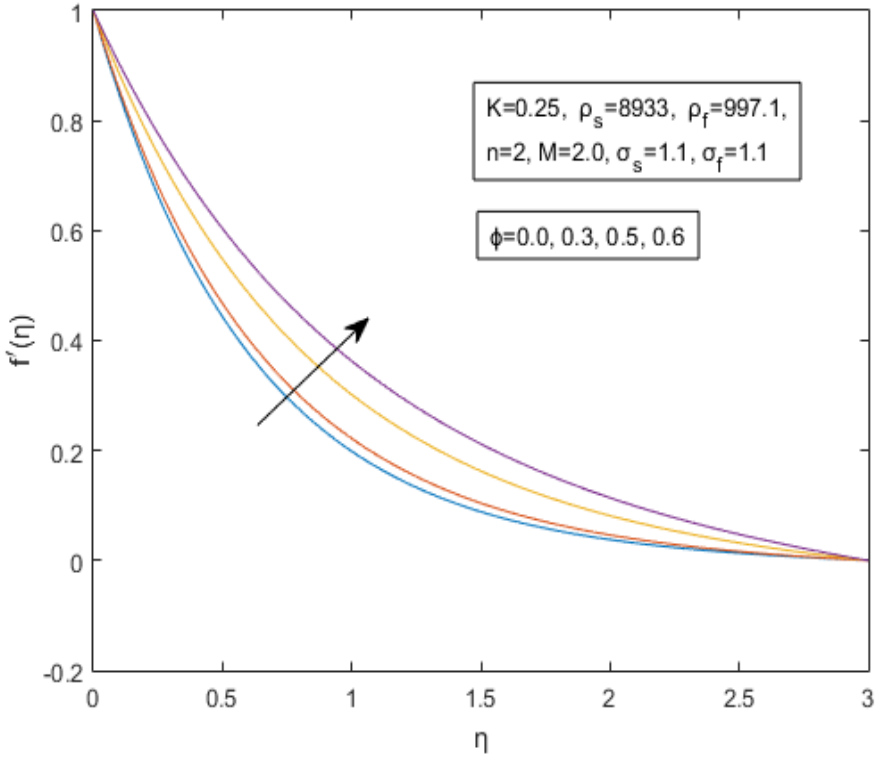

FIGURE 3.2: Impact of ϕ on $f'(\eta)$ when M=2

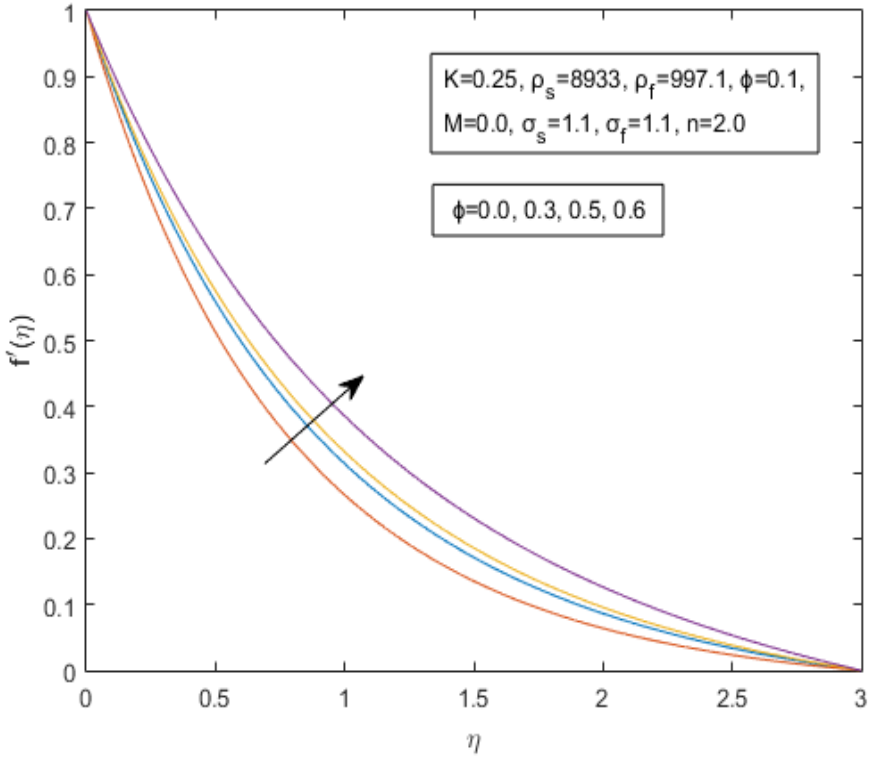

FIGURE 3.3: Impact of ϕ on $f'(\eta)$ when M=0

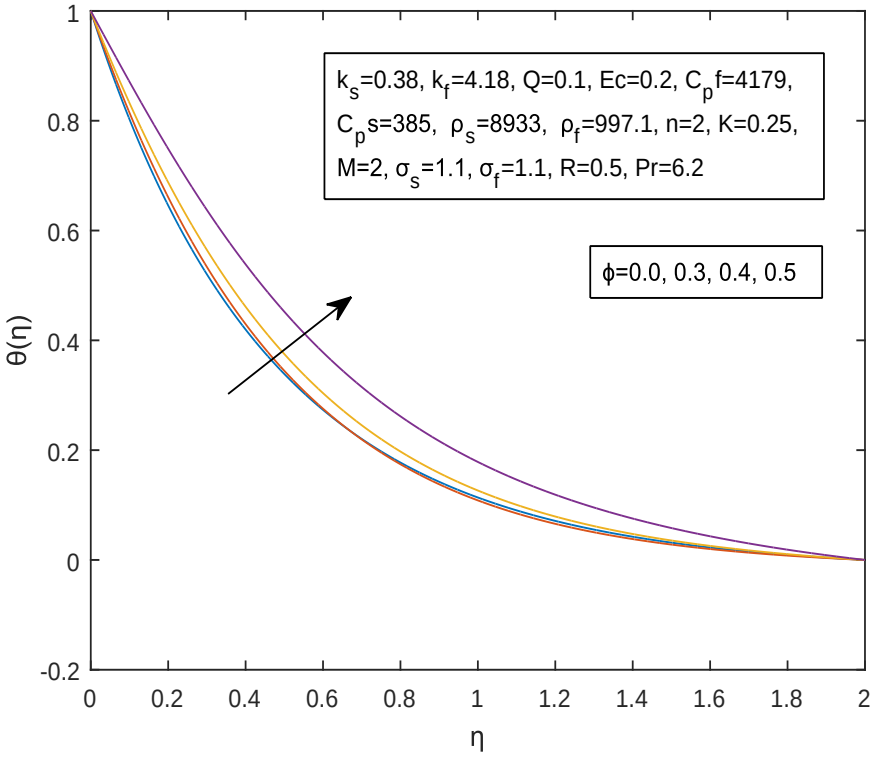

FIGURE 3.4: Impact of ϕ on temperature profile when M=2

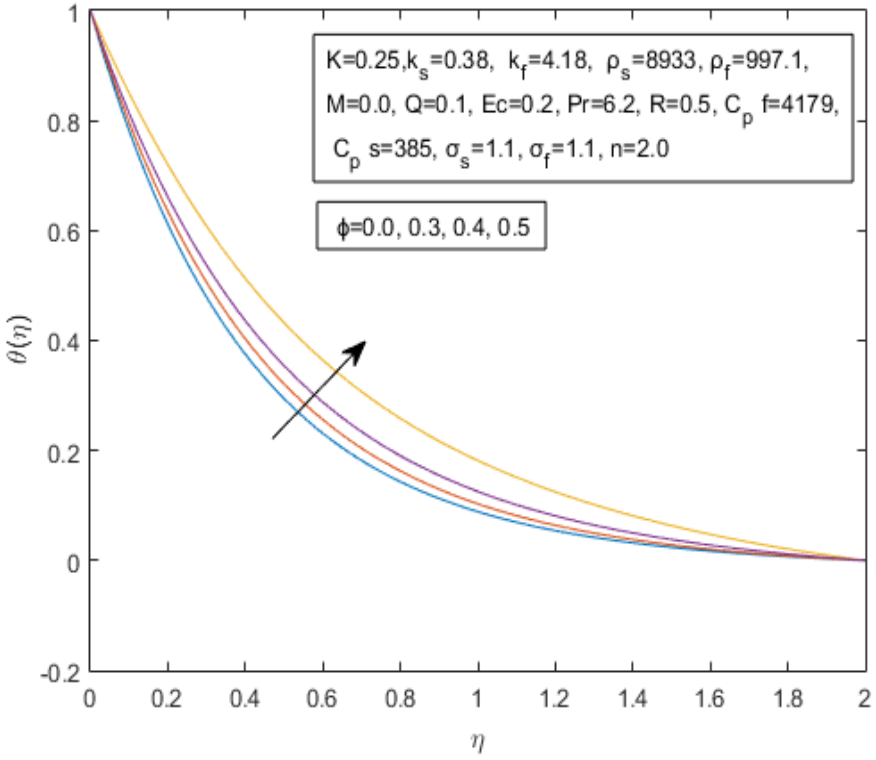

FIGURE 3.5: Impact of ϕ on temperature profile when M=0

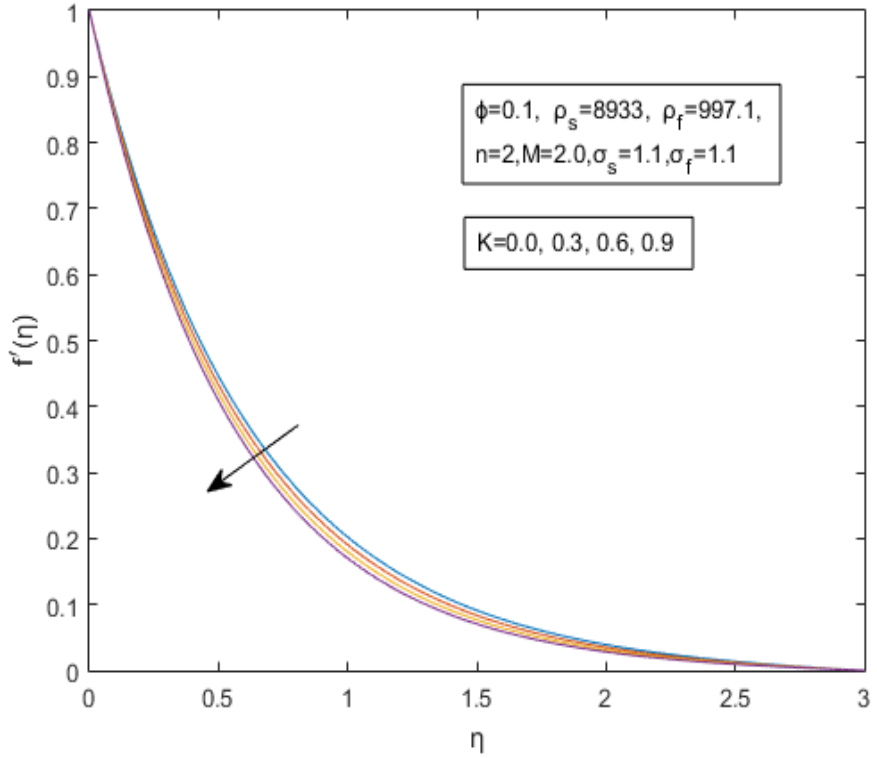

FIGURE 3.6: Impact of K on $f'(\eta)$

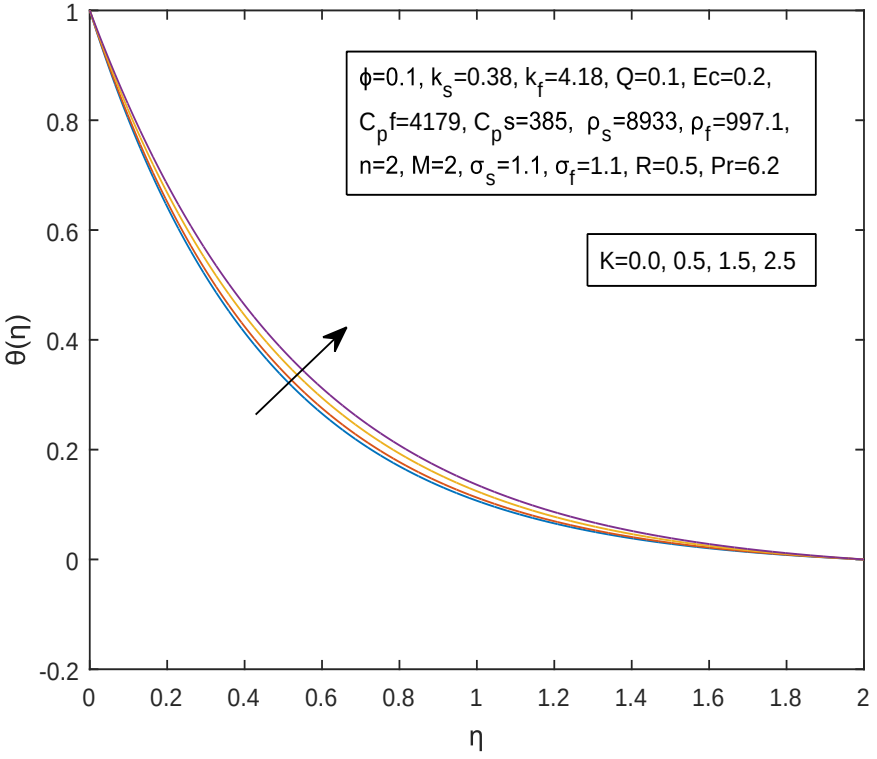

FIGURE 3.7: Impact of K on temperature profile

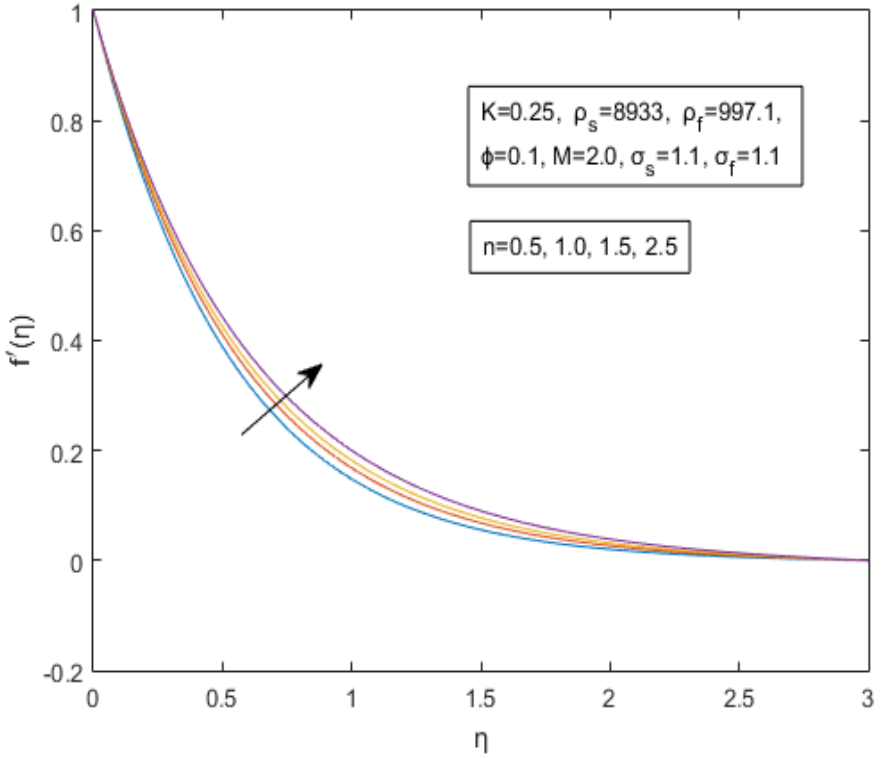

FIGURE 3.8: Impact of n on $f'(\eta)$

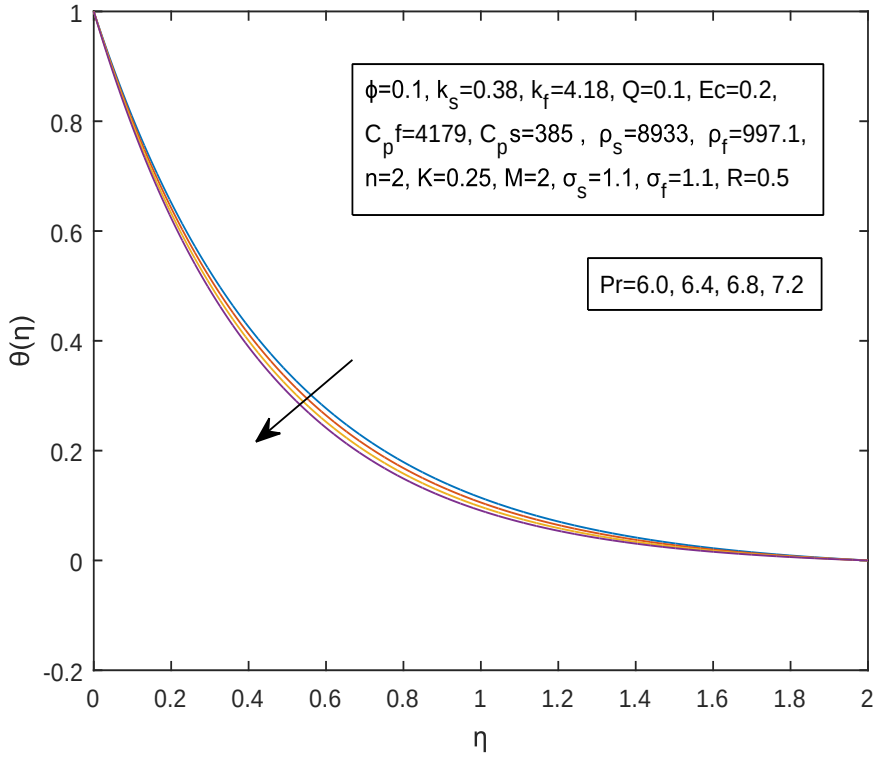

FIGURE 3.9: Impact of Pr on the temperature profile.

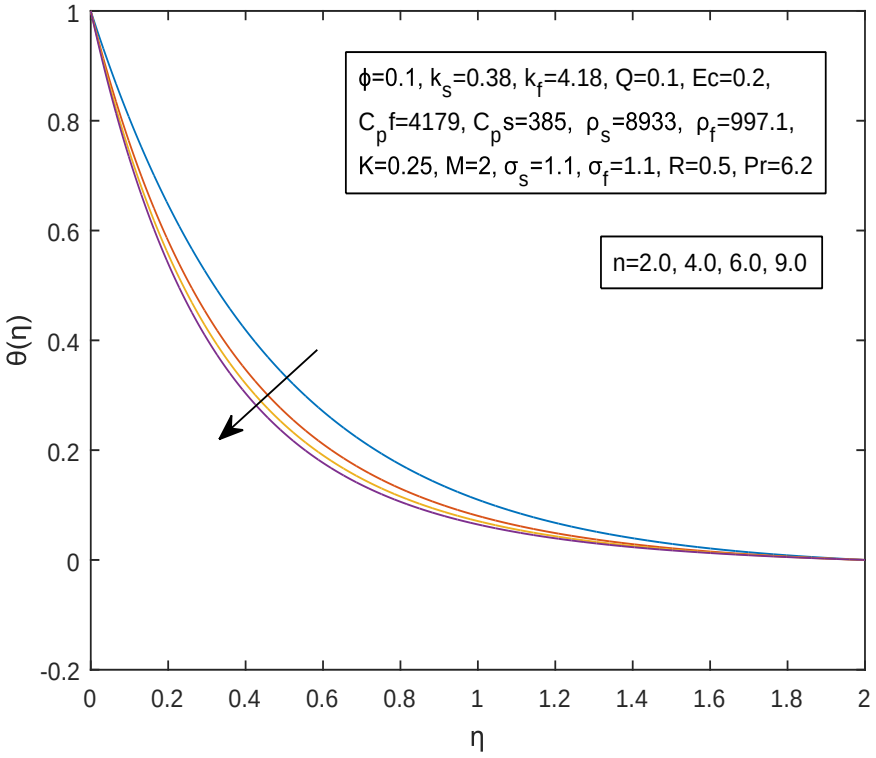

FIGURE 3.10: Impact of n on the temperature profile

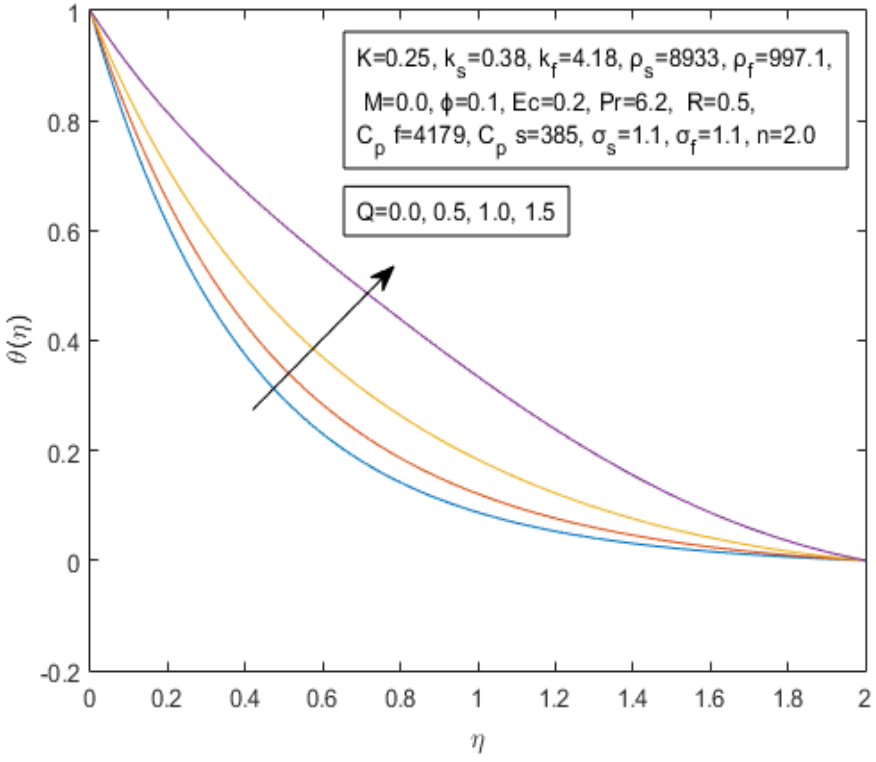

FIGURE 3.11: Impact of Q on temperature profile

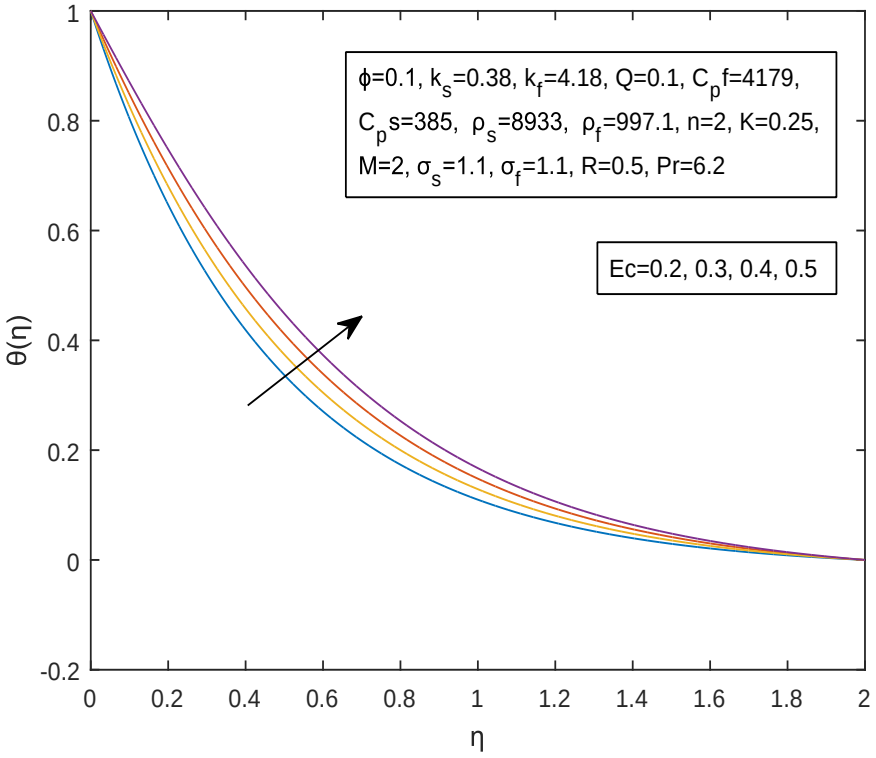

FIGURE 3.12: Impact of Ec on the temperature profile

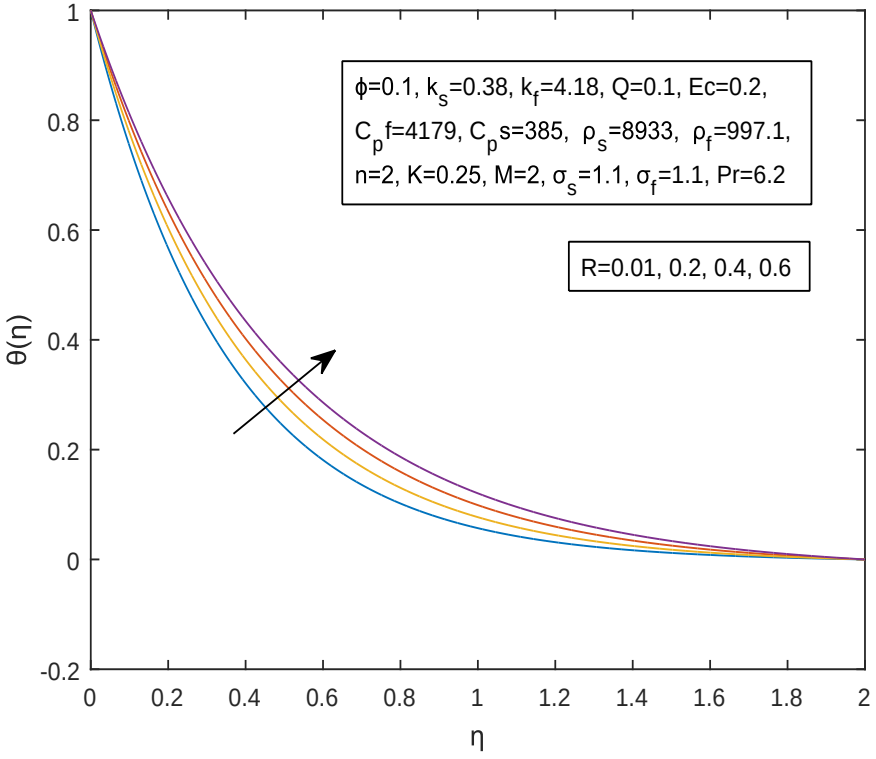

FIGURE 3.13: Impact of R on the temperature profile

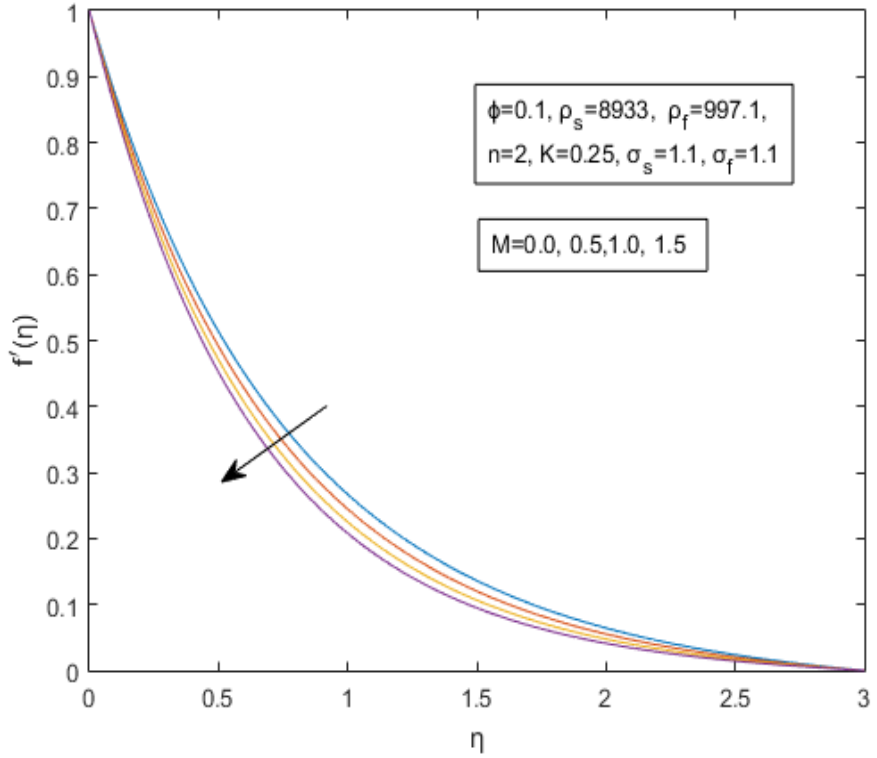

FIGURE 3.14: Impact of M on $f'(\eta)$

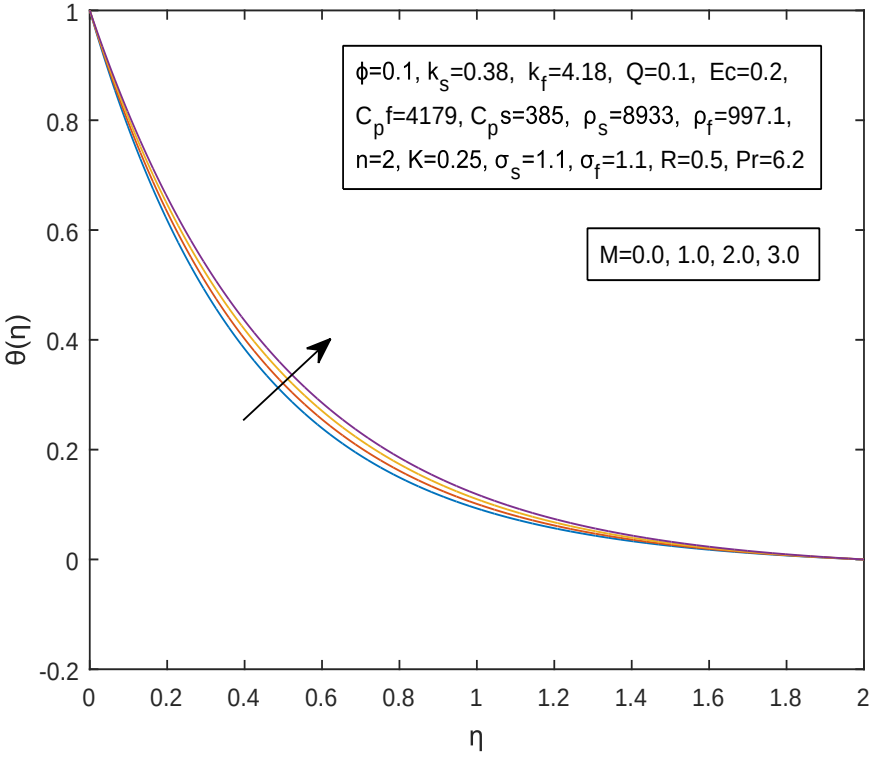

FIGURE 3.15: Impact of M on temperature profile

Chapter 4

MHD Radiative Hybrid Nanofluid Flow with Inclined Magnetic Field

4.1 Introduction

This chapter extends the work of [25] by including hybrid nanofluid with an inclined magnetic field. The similarity transformations are used to turn the controlling nonlinear PDEs into a system of dimensionless ODEs. Applying the numerical method known as the shooting method yields the numerical solution of ODEs. The final results for important parameters affecting $f'(\eta)$ and $\theta(\eta)$ .Tthe detailed discussion of these tables and graphs, appears at the end of this chapter.

4.2 Mathematical Modeling

This section is dedicated to analyse the two-dimensional, MHD flow of hybrid-nanofluid past a porous medium and nonlinear stretching sheet. The Titanium TiO_2 and Copper Cu are considered as hybrid nanoparticles and water as base fluid. The area $y > 0$ was occupied by the flow. A magnetic field of force B

is applied with the horizantal axis inclined at a γ angle. Additionally, the flow direction is considered as the x-axis and the y-axis is normal to it (See Figure 3.1).

4.2.1 The Governing Equations

The governing model for the above problem is

$$\frac{\partial u}{\partial x}+\frac{\partial v}{\partial y}=0, \tag{4.1}$$

$$\rho_{hnf}\left(u\frac{\partial u}{\partial x}+v\frac{\partial u}{\partial y}\right)=\mu_{hnf}\left(\frac{\partial^2 u}{\partial y^2}\right)-\frac{\mu_{hnf}}{k(x)}u-\sigma_{hnf}B^2(x)\sin^2(\gamma)u, \tag{4.2}$$

$$\begin{aligned}u\frac{\partial T}{\partial x}+v\frac{\partial T}{\partial y}=\alpha_{hnf}\left(\frac{\partial^2 T}{\partial y^2}\right)+\frac{\mu_{hnf}}{(\rho C_p)_{hnf}}\left(\frac{\partial u}{\partial y}\right)^2-\frac{1}{(\rho C_p)_{hnf}}\left(\frac{\partial q_r}{\partial y}\right)\\ +\frac{q}{(\rho C_p)_{hnf}}(T-T_\infty).\end{aligned} \tag{4.3}$$

alongwith the following boundary conditions;

$$\left.\begin{aligned}&u=U_w(x)=ax^n, \quad v=0, \quad T=T_w, \quad at \quad y=0.\\ &u\to 0, \quad T\to T_\infty, \quad as \quad y\to\infty.\end{aligned}\right\} \tag{4.4}$$

4.2.2 Similarity Transformations

The following similarity transformations will be used to transform (4.1)-(4.4) into a system of ODEs:

$$\left.\begin{aligned}\psi(x,y)&=\sqrt{\frac{2\nu_f a}{n+1}}x^{\frac{n+1}{2}}f(\eta),\\ \eta&=y\sqrt{\frac{a(n+1)}{2\nu_f}}x^{\frac{n-1}{2}},\\ \theta(\eta)&=\frac{T-T_\infty}{T_w-T_\infty},\end{aligned}\right\} \tag{4.5}$$

where ψ stands for the stream function, η denotes the similarity independent variable, f' and θ are the dimensionless velocity and temperature profiles. The

thermophysical properties of hybrid nanofluid are stated as follow [38]:

$$\rho_{hnf} = \left[(1-\phi_2)\left((1-\phi_1)\rho_f + \phi_1\rho_{s1}\right)\right] + \phi_2\rho_{s2},$$
$$\mu_{hnf} = \frac{\mu_f}{(1-\phi_1)^{2.5}(1-\phi_2)^{2.5}},$$
$$(\rho C_p)_{hnf} = (1-\phi_2)\left((1-\phi_1)(\rho C_p)_f + \phi_1(\rho C_p)_{s1}\right) + \phi_2(\rho C_p)_{s2},$$
$$\frac{k_{hnf}}{k_f} = \frac{k_{s2}+2k_{nf}-2\phi_2(2k_{nf}-k_{s2})}{k_{s2}+2k_{nf}+2\phi_2(2k_{nf}-k_{s2})}.\frac{k_{s1}+2k_f-2\phi_1(2k_f-k_{s1})}{k_{s1}+2k_f+2\phi_1(2k_f-k_{s1})},$$
$$\frac{\sigma_{hnf}}{\sigma_f} = 1 + \frac{3\left[\frac{\sigma_{s1}\phi_1+\sigma_{s2}\phi_2}{\sigma_f} - (\phi_1+\phi_2)\right]}{\left(2+\frac{\sigma_{s1}+\sigma_{s2}}{\sigma_f}\right) - \left(\frac{\sigma_{s1}\phi_1+\sigma_{s2}\phi_2}{\sigma_f}\right) + (\phi_1+\phi_2)},$$
$$\alpha_{hnf} = \frac{k_{hnf}}{(\rho Cp_)hnf}.$$

where ϕ_1, ϕ_2, ρ_{s1}, ρ_{s2}, ρ_{hnf}, μ_{hnf}, $(\rho C_P)_{s1}$, $(\rho C_P)_{s2}$, $(\rho C_P)_{hnf}$, k_{hnf}, k_{s1}, k_{s2}, α_{hnf} are respectivly the nanoparticles solid volume fraction of Titanium, nanoparticles solid volume fraction of Copper,the density of the solid nanoparticles of Titanium, the density of the solid nanoparticles of Copper, the density of hybrid nanofluid, the viscosity of hybrid nanofluid, the heat capacitance of Titanium nanoparticles, the heat capacitance of Copper nanoparticles, the heat capacitance of hybrid-nanofluid, the thermal conductivity of the hybridnanofluid, the thermal conductivity of the Titanium nanoparticles and the thermal conductivity of the Copper nanoparticles and the thermal diffusivity of the hybrid nanofluid.

4.3 Transformation of PDEs into ODEs

4.3.1 The Governing Equation

Here, the transformation of (4.1)-(4.3) into a system of ODEs using the similarity transformation will be discussed. The verification of the continuity equation through similarity transformation is already discussed in chapter 3. Now, the conversion of (4.2) into the dimensionless form will be discussed. The required

derivatives are already calculated in chapter 3. By using those values:

$$\rho_{hnf}a^2x^{2n-1}\left(nf'^2(\eta)-\frac{(n+1)}{2}f(\eta)f''(\eta)\right)=\mu_{hnf}a^2x^{2n-1}\left(\frac{n+1}{2\nu}\right)f'''(\eta)$$
$$-\mu_{hnf}\frac{a^2x^{2n-1}f'(\eta)K}{\nu_f}-\sigma_{hnf}ax^{2n-1}\sin^2\gamma B_0^2f'(\eta).$$
$$\Rightarrow \rho_{hnf}a^2x^{2n-1}\left(\frac{n+1}{2}\right)\left[\left(\frac{2n}{n+1}\right)f'(\eta)-f(\eta)f''(\eta)\right]=\mu_{hnf}a^2x^{2n-1}\left(\frac{n+1}{2\nu}\right).$$
$$\left[f'''(\eta)-\left(\frac{2\nu}{n+1}\right)\left(\frac{K}{\nu}+\sin^2\gamma\frac{\sigma_{hnf}}{\mu_{hnf}}\frac{B_0^2}{a}\right)f'(\eta)\right].$$
$$\Rightarrow \nu\frac{\rho_{hnf}}{\mu_{hnf}}\left(\frac{n+1}{2}\right)\left[\left(\frac{2n}{n+1}\right)f'(\eta)-f(\eta)f''(\eta)\right]=f'''(\eta)-\left(\frac{2}{n+1}\right)f'(\eta)$$
$$\left[K+\sin^2\gamma\nu\frac{\sigma_{hnf}}{\mu_{hnf}}\frac{B_0^2}{a}\right].$$
$$\Rightarrow f'''(\eta)+(1-\phi_1)^{2.5}(1-\phi_2)^{2.5}\left[(1-\phi_2)\left(1-\phi_1+\phi_1\left(\frac{\rho_{s1}}{\rho_f}\right)+\phi_2\frac{\rho_{s2}}{\rho_f}\right)\right]$$
$$\left(f(\eta)f''(\eta)-\frac{2n}{n+1}\right)-\left(\frac{2}{n+1}\right)f'(\eta)\left[K+M\sin^2\gamma(1-\phi_1)^{2.5}(1-\phi_2)^{2.5}\right.$$
$$\left.\left(1+\frac{3\left[\frac{\sigma_{s1}\phi_1+\sigma_{s2}\phi_2}{\sigma_f}-(\phi_1+\phi_2)\right]}{\left(2+\frac{\sigma_{s1}+\sigma_{s2}}{\sigma_f}\right)-\left(\frac{\sigma_{s1}\phi_1+\sigma_{s2}\phi_2}{\sigma_f}\right)+(\phi_1+\phi_2)}\right)\right]=0.$$
$$\Rightarrow f'''(\eta)=-(1-\phi_1)^{2.5}(1-\phi_2)^{2.5}\left[(1-\phi_2)\left(1-\phi_1+\phi_1\left(\frac{\rho_{s1}}{\rho_f}\right)+\phi_2\frac{\rho_{s2}}{\rho_f}\right)\right]$$
$$\left(f(\eta)f''(\eta)-\frac{2n}{n+1}\right)+\left(\frac{2}{n+1}\right)f'(\eta)\left[K+M\sin^2\gamma(1-\phi_1)^{2.5}(1-\phi_2)^{2.5}\right.$$
$$\left.\left(1+\frac{3\left[\frac{\sigma_{s1}\phi_1+\sigma_{s2}\phi_2}{\sigma_f}-(\phi_1+\phi_2)\right]}{\left(2+\frac{\sigma_{s1}+\sigma_{s2}}{\sigma_f}\right)-\left(\frac{\sigma_{s1}\phi_1+\sigma_{s2}\phi_2}{\sigma_f}\right)+(\phi_1+\phi_2)}\right)\right].$$

Let

$$A=\left[(1-\phi_2)\left(1-\phi_1+\phi_1\left(\frac{\rho_{s1}}{\rho_f}\right)+\phi_2\frac{\rho_{s2}}{\rho_f}\right).\right.$$
$$B=\left(1+\frac{3\left[\frac{\sigma_{s1}\phi_1+\sigma_{s2}\phi_2}{\sigma_f}-(\phi_1+\phi_2)\right]}{\left(2+\frac{\sigma_{s1}+\sigma_{s2}}{\sigma_f}\right)-\left(\frac{\sigma_{s1}\phi_1+\sigma_{s2}\phi_2}{\sigma_f}\right)+(\phi_1+\phi_2)}\right).$$
$$\Rightarrow f'''(\eta)=-(1-\phi_1)^{2.5}(1-\phi_2)^{2.5}A\left(f(\eta)f''(\eta)-\frac{2n}{n+1}\right)$$
$$+\left(\frac{2}{n+1}\right)f'(\eta)\left[K+M\sin^2\gamma(1-\phi_1)^{2.5}(1-\phi_2)^{2.5}B.\right. \qquad (4.6)$$

Now, for the procedure for the conversion of equation (4.3) into the dimensionless form useful derivatives are picked from chapter 3 to plug in the following manner.

$$abx^{3n-2}\left[2n-1f'(\eta)\theta-\frac{n+1}{2}\theta' f(\eta)\right]=\alpha_{hnf}\frac{ab(n+1)}{2\nu}x^{3n-2}\theta''$$
$$+\frac{\mu_{hnf}}{(\rho Cp)_{hnf}}\frac{a^3(n+1)}{2\nu}f''^2(\eta)x^{3n-1}-\frac{1}{(\rho Cp)_{hnf}}\frac{16\sigma*}{3k*}T_\infty^3\frac{ab(n+1)}{2\nu}x^{3n-2}\theta''$$
$$-\frac{q}{(\rho Cp)_{hnf}}\left(T-T_\infty\right).$$
$$\Rightarrow(2n-1)f'(\eta)\theta-(\frac{n+1}{2})\theta' f(\eta)=\frac{k_{hnf}}{(\rho Cp)_{hnf}}\frac{n+1}{2v}\theta''$$
$$-\frac{1}{(\rho Cp)_{hnf}}\frac{16\sigma*}{3k*}T_\infty^3\frac{(n+1)x}{2\nu}\theta''+\frac{\mu_{hnf}}{(\rho Cp)_{hnf}}\frac{a^3(n+1)x}{2\nu b}f''^2(\eta)$$
$$-q(\rho Cp)_{hnf}x^{1-n}\theta.$$
$$\Rightarrow\theta''+\frac{16\sigma*}{k_{nf}3k*}T_\infty^3\theta''+\frac{\mu_{hnf}a^2}{k_{hnf}b}xf''-\frac{2(2n-1)}{n+1}\frac{(\rho Cp)_{hnf}}{k_{hnf}}\nu f'\theta$$
$$+\frac{(\rho Cp)_{hnf}}{k_{hnf}}\nu f'\theta+\frac{2q\nu x^{1-n}}{k_{hnf}a(n+1)}\theta=0.$$
$$\Rightarrow\theta''+\frac{4R}{3}\theta''+\frac{\mu_{hnf}a^2x}{k_{hnf}b}f''-\frac{2(2n-1)}{n+1}\frac{(\rho Cp)_{hnf}}{k_{hnf}}\nu f'\theta+\frac{(\rho Cp)_{hnf}}{k_{hnf}}\nu f'\theta$$
$$+\frac{2q\nu x^{1-n}}{k_{hnf}a(n+1)}\theta=0.$$
$$\Rightarrow\theta''\left(1+\frac{4R}{3}\right)+\frac{\mu_f a^2x}{k_{hnf}b(1-\phi_-1)^{2.5}(1-\phi_2)^{2.5}}(f'')^2$$
$$+\left(f\theta'-\frac{2(2n-1)}{n+1}f'\theta\right)\frac{\alpha(\rho Cp)_{hnf}\nu}{k_{hnf}\alpha}+\left(\frac{2}{n+1}\right)\frac{qx\nu}{k_{hnf}ax^n}\theta=0.$$
$$\Rightarrow\theta''\left(1+\frac{4R}{3}\right)+\frac{\nu\rho a^2x}{k_{nf}b(1-\phi_1)^{2.5}(1-\phi_2)^{2.5}}(f'')^2$$
$$+\left(f\theta'-\frac{2(2n-1)}{n+1}f'\theta\right)\frac{\nu}{\alpha}\frac{\alpha(\rho Cp)_{hnf}}{k_{hnf}}+\frac{2}{n+1}\frac{qx}{k_{nf}(\rho Cp)_f}\nu(\rho Cp)_f\theta=0.$$
$$\Rightarrow\theta''\left(1+\frac{4R}{3}\right)+\frac{k}{k_{hnf}}\frac{\nu}{\alpha}\frac{a^2x^{2n-1}}{(\rho Cp)_f b(1-\phi_1)^{2.5}(1-\phi_2)^{2.5}x^{2n-1}}(f'')^2$$
$$+\frac{k}{k_{hnf}}\left(f\theta'-\left(\frac{2(2n-1)}{n+1}\right)f'\theta\right)\frac{\nu}{\alpha}\frac{(\rho Cp)_{hnf}}{(\rho Cp)_f}$$
$$+\frac{k}{k_{hnf}}\left(\frac{2}{n+1}\right)\frac{qx}{(\rho Cp)_f ax^n}\frac{\nu}{\alpha}\theta=0.$$
$$\Rightarrow\frac{k_{nf}}{k_f}\left(1+\frac{4R}{3}\right)\theta''+P_r\left(\frac{E_c}{(1-\phi_1)^{2.5}(1-\phi_2)2.5}\right)(f'')^2$$
$$+\left(f\theta'-\left(\frac{2(2n-1)}{n+1}\right)f'\theta\right)$$
$$P_r\left((1-\phi_2)\left(1+\phi_1+\phi_1\frac{(\rho Cp)_{s1}}{(\rho Cp)_f}+\phi_2\frac{(\rho Cp)_{s2}}{(\rho Cp)_f}\right)\right)+\left(\frac{2}{n+1}\right)Q\theta=0.$$

$$\Rightarrow \theta'' = \left(\frac{k_f}{k_{nf}}\right)\frac{1}{\left(1+\frac{4R}{3}\right)}\left[P_r\left(\frac{E_c}{(1-\phi_1)^{2.5}(1-\phi_2)2.5}\right)(f'')^2 + \left(f\theta' - \left(\frac{2(2n-1)}{n+1}\right)f'\theta\right) P_r\left((1-\phi_2)\left(1+\phi_1+\phi_1\frac{(\rho Cp)_{s1}}{(\rho Cp)_f}+\phi_2\frac{(\rho Cp)_{s2}}{(\rho Cp)_f}\right)\right) + \left(\frac{2}{n+1}\right)Q\theta\right].$$

Let

$$C = \left((1-\phi_2)\left(1+\phi_1+\phi_1\frac{(\rho Cp)_{s1}}{(\rho Cp)_f}+\phi_2\frac{(\rho Cp)_{s2}}{(\rho Cp)_f}\right)\right).$$

$$\Rightarrow \theta'' = -\left(\frac{k_f}{k_{nf}}\right)\frac{1}{\left(1+\frac{4R}{3}\right)}\left[P_r\left(\frac{E_c}{(1-\phi_1)^{2.5}(1-\phi_2)2.5}\right)(f'')^2 - \left(f\theta' - \left(\frac{2(2n-1)}{n+1}\right)f'\theta\right)P_rC + \left(\frac{2}{n+1}\right)Q\theta\right]. \tag{4.7}$$

The dimensionless form of the governing model is

$$\Rightarrow f'''(\eta) + (1-\phi_1)^{2.5}(1-\phi_2)^{2.5}A\left(f(\eta)f''(\eta) - \frac{2n}{n+1}\right) - \left(\frac{2}{n+1}\right)f'(\eta)\left[K + M\sin^2\gamma(1-\phi_1)^{2.5}(1-\phi_2)^{2.5}B\right] = 0. \tag{4.8}$$

$$\Rightarrow \theta'' + \left(\frac{k_f}{k_{nf}}\right)\frac{1}{\left(1+\frac{4R}{3}\right)}\left[P_r\left(\frac{E_c}{(1-\phi_1)^{2.5}(1-\phi_2)2.5}\right)(f'')^2 + \left(f\theta' - \left(\frac{2(2n-1)}{n+1}\right)f'\theta\right)P_rC + \left(\frac{2}{n+1}\right)Q\theta\right] = 0. \tag{4.9}$$

The detailed discussion for the transformation of (4.5) into the dimentionless form have been done in Chapter 3. Hence utilizing those as follows:

$$\left.\begin{aligned} &f(0) = 0, \quad f'(0) = 1, \quad \theta(0) = 1. \\ &f'(\infty) \to 0, \quad \theta(\infty) \to 0. \end{aligned}\right\} \tag{4.10}$$

For, the conversion of dimentional physical parameter into non dimentional some necessary derivations are given below. The dimentional form of skin fraction coefficient is,

$$C_f = \frac{\tau_w|_{y=0}}{\rho_f U_w^2(x)}.$$

The steps listed below can help to achieve the dimensionless form of C_f.

Since

$$\tau_w = \mu_{hnf}\left(\frac{\partial u}{\partial y}\right)_{y=0}.$$

$$\Rightarrow C_f = \frac{\mu_{hnf}}{\rho_f u_w^2}\left(\frac{\partial u}{\partial y}\right)_{y=0}.$$

$$\Rightarrow \left(\frac{\partial u}{\partial y}\right) = ax^n f''(\eta)\sqrt{\frac{a(n+1)}{2\nu}}x^{\frac{n-1}{2}}.$$

$$\Rightarrow C_f = \frac{\mu_{hnf}}{\rho_f u_w^2}ax^n f''(\eta)\sqrt{\frac{a(n+1)}{2\nu}}x^{\frac{n-1}{2}},$$

$$= \frac{\mu_f}{\rho_f u_w^2(1-\phi_1)^{2.5}(1-\phi_2)^{2.5}}ax^{\frac{3n-1}{2}}f''(\eta)\sqrt{\frac{a(n+1)}{2\nu}},$$

$$= \frac{\rho_f \nu}{\rho_f a^2 x^{2n}(1-\phi_1)^{2.5}(1-\phi_2)^{2.5}}ax^{\frac{3n-1}{2}}f''(\eta)\sqrt{\frac{a(n+1)}{2\nu}},$$

$$= \frac{v^{\frac{1}{2}}}{(1-\phi_1)^{2.5}(1-\phi_2)^{2.5}a^{\frac{1}{2}}x^{\frac{n+1}{2}}}f''(\eta)\sqrt{\frac{(n+1)}{2}},$$

$$= \frac{1}{(1-\phi_1)^{2.5}(1-\phi_2)^{2.5}Re_x^{\frac{1}{2}}}f''(\eta)\left(\frac{n+1}{2}\right).$$

Hence, the dimentionless form of the skin friction cofficient is,

$$\Rightarrow C_f Re_x^{\frac{1}{2}} = \frac{1}{(1-\phi_1)^{2.5}(1-\phi_2)^{2.5}}f''(0)\left(\frac{n+1}{2}\right), \tag{4.11}$$

where Re denotes the Renold number which is defind as $Re_x = \frac{xu_x(x)}{\nu_f}$.

Now the dimentionless form of local Nusselt number will be derived.

$$Nu_x = \frac{xq_w}{k_f(T_w - T_\infty)}.$$

$$q_w = \left(-\left(k_{nf} + \frac{16\sigma^* T_\infty^3}{3k^*}\right)\left(\frac{\partial T}{\partial y}\right)\right)_{y=0}.$$

$$\Rightarrow \left(\frac{\partial T}{\partial y}\right) = (T_w - T_\infty)\,\theta'(\eta)\sqrt{\frac{a(n+1)}{2\nu}}x^{\frac{n-1}{2}}.$$

$$
\begin{aligned}
\Rightarrow Nu_x &= -\frac{x\left(k_{hnf}+\frac{16\sigma^* T_\infty^3}{3k^*}\right)\left(\frac{\partial T}{\partial y}\right)_{y=0}}{k_f(T_w-T_\infty)}. \\
&= -\frac{x\left(k_{hnf}+\frac{16\sigma^* T_\infty^3}{3k^*}\right)}{k_f(T_w-T_\infty)}\left(T_w-T_\infty\right)\theta'(\eta)\sqrt{\frac{a(n+1)}{2\nu}}x^{\frac{n-1}{2}}, \\
&= -\frac{k_{hnf}}{k_f}\left(1+\frac{4}{3}R\right)x^{\frac{n+1}{2}}\theta'\left(\frac{a(n+1)}{2\nu}\right)^{\frac{1}{2}}, \\
&= -\frac{k_{hnf}}{k_f}\left(1+\frac{4}{3}R\right)\theta'\left(\frac{n+1}{2}\right)^{\frac{1}{2}}\left(\frac{ax^{n+1}}{2\nu}\right)^{\frac{1}{2}}, \\
&= -\frac{k_{hnf}}{k_f}\left(1+\frac{4}{3}R\right)\sqrt{\frac{n+1}{2}}\theta'(\eta)Re_x^{\frac{1}{2}}.
\end{aligned}
$$

Hence, the Nusselt number in non dimentional form will be:

$$
\Rightarrow Re_x^{\frac{-1}{2}}Nu_x = -\frac{k_{hnf}}{k_f}\left(1+\frac{4}{3}R\right)\left(\frac{n+1}{2}\right)^{\frac{1}{2}}\theta'(0),
$$

where Reynolds number Re is represented by the equation $Re_x = \frac{xu_x(x)}{\nu_f}$.

4.4 Solution Methodology

The shooting method has been applied for the solution of the ordinary differential equation (4.8). The following notations have been taken into account:

$$
f = Y_1, \qquad f' = Y_1' = Y_2, \qquad f'' = Y_1'' = Y_2' = Y_3, \qquad f''' = Y_3'.
$$

The momentum equation is then transformed into the system of first order ODEs as shown below.

$$
\begin{aligned}
&Y_1' = Y_2, && Y_1(0) = 0. \\
&Y_2' = Y_3, && Y_2(0) = 1. \\
&Y_3' = -(1-\phi_1)^{2.5}(1-\phi_2)^{2.5}A\left(Y_1Y_3 - \frac{2n}{n+1}Y_2^2\right) \\
&\quad -\left(\frac{2}{n+1}\right)Y_2\left[K + M\sin^2\gamma(1-\phi_1)^{2.5}(1-\phi_2)^{2.5}B\right], && Y_3(0) = s.
\end{aligned}
$$

where,

$$A = \Bigg[(1-\phi_2)\Bigg(1-\phi_1+\phi_1\left(\frac{\rho_{s1}}{\rho_f}\right)+\phi_2\frac{\rho_{s2}}{\rho_f}\Bigg).$$

$$B = \left(1+\frac{3\left[\frac{\sigma_{s1}\phi_1+\sigma_{s2}\phi_2}{\sigma_f}-(\phi_1+\phi_2)\right]}{\left(2+\frac{\sigma_{s1}+\sigma_{s2}}{\sigma_f}\right)-\left(\frac{\sigma_{s1}\phi_1+\sigma_{s2}\phi_2}{\sigma_f}\right)+(\phi_1+\phi_2)}\right).$$

Runge-Kutta method of order 4 have been used to solve the aforementioned IVP. Choose the missing condition s in such a way that:

$$Y_2(\eta_\infty, s) = 0.$$

To determine s, Newton's method will be applied. The iterative structure for this method is as follow:

$$s^{n+1} = s^n - \frac{Y_2(\eta_\infty, s)}{\frac{\partial}{\partial s}Y_2(\eta_\infty, s)}$$

We also introduce the following notations.

$$\frac{\partial Y_1}{\partial s} = Y_4 \qquad \frac{\partial Y_2}{\partial s} = Y_5 \qquad \frac{\partial Y_3}{\partial s} = Y_6.$$

The form of the Newton's iterative scheme changes as a result of these new notations.

$$s^{n+1} = s^n - \frac{Y_2(\eta_\infty, s)}{Y_5(\eta_\infty, s)}.$$

We now obtain three more of ODEs by differentiating the system of three first order ODEs with w.r.t. to s.

$$Y_4' = Y_5, \qquad Y_4(0) = 0.$$

$$Y_5' = Y_6, \qquad Y_5(0) = 0.$$

$$Y_6' = -(1-\phi_1)^{2.5}(1-\phi_2)^{2.5}A\left(Y_1Y_6 - \frac{2n}{n+1}\right)2Y_2Y_5$$
$$-\left(\frac{2}{n+1}\right)Y_5\Bigg[K + M\sin^2\gamma(1-\phi)^{2.5}(1-\phi_2)^{2.5}B\Bigg], \qquad Y_6(0) = 1.$$

Following threshold is set for the approximation of numerical results.

$$\mid Y_2(\xi_\infty, s) \mid < \epsilon,$$

where ϵ is an arbitrarily small positive number. The value ofϵ is takes been 10^{-10} throughout this chapter.

After obtaining the numerical solution for f, equation (4.9) is solved by incoprating the shooting technique again .Since, in equation (4.9) θ is coupled with f here we utilize the previously obtained numerical solution .Following notations are used for this purpose.

$$\theta = Z_1, \qquad \theta' = Z_1' = Z_2, \qquad \theta'' = Z_2'$$

As a result, the energy equation (4.9) is converted into the following system of first order ODEs.

$$\begin{aligned} Z_1' &= Z_2, && Z_1(0) = 1. \\ Z_2' &= \frac{k_f}{k_{hnf}\left(1+\frac{4}{5}R\right)}\Bigg[- P_r\left(\frac{E_c}{(1-\phi)^{2.5}(1-\phi_2)^{2.5}}\right)(f'')^2 \\ &\quad - \left(f\theta' - \left(\frac{2(2n-1)}{n+1}\right) f' Z_2\right) P_r C - \left(\frac{2}{n+1}\right) Q Z_1\Bigg], && Z_2(0) = t. \end{aligned}$$

where,

$$C = \left((1-\phi_2)\left(1+\phi_1+\phi_1\frac{(\rho Cp)_{s1}}{(\rho Cp)_f}+\phi_2\frac{(\rho Cp)_{s2}}{(\rho Cp)_f}\right)\right).$$

The above initial value problem (IVP) will be numerically solved by RK-4 technique. The missing condition t in the aforementioned starting value problem must meet the following relation.

$$Z_1(\eta_\infty, t) = 0.$$

The Newton's iterative method will be used to find the missing initial condition for convergent numerical results.

$$t^{n+1} = t^n - \frac{Y_1(\eta_\infty, t)}{\dfrac{\partial Y_1(\eta_\infty, t)}{\partial t}}.$$

We further introduce the following notations,

$$\frac{\partial Z_1}{\partial t} = Z_3 \qquad\qquad \frac{\partial Z_2}{\partial Z} = Z_4.$$

Following two ODEs are obtained by differentiating the system of two first order ODEs with regard to t.

$$\begin{aligned} Z_3' &= Z_4 && Z_3(0) = 0 \\ Z_4' &= -\frac{k_f}{k_{hnf}\left(1+\frac{4}{5}R\right)}\left[- P_r\left(\frac{E_c}{(1-\phi_1)^{2.5}(1-\phi_2)}\right)(f'')^2 \right. \\ &\quad \left. - \left(f\theta' - \left(\frac{2(2n-1)}{n+1}\right) f' Z_2\right) P_r C - \left(\frac{2}{n+1}\right) Q Z_1 \right] && Z_4(0) = 1. \end{aligned}$$

The stoping criteria for shooting method's is defined as following:

$$\mid Z_1(\eta_\infty, t) \mid < 10^{-10}.$$

4.5 Representation of Graphs and Tables

The main goal of this study is to investigate the effect of various parameters on velocity and temperature profile as well as on the skin fraction coefficient and Nusselt number. Through graphs and tables, the effect of variation of various dimentionless parameters are depicted, including nonlinear stretching parameter, magnetic parameter, thermal radiation parameter and nanoparticle volume fraction. Table 4.1 and 4.2 display the numerical results for the skin friction coefficient and local Nusselt number for various values of dimentionless parameters.

4.5.1 Skin Friction Coefficient

The influence of the nanoparticle volume friction, magnetic parameter, nonlinear sheet parameter and permeability parameter on the skin friction coefficient is shown in Table 4.1. The following discoveries have been made.

- As the nanoparticle volume friction ϕ_1 and ϕ_2 increases, so does the skin friction coefficient.
- The skin friction coefficient decreases as the magnetics parameter's values increase..

The interval I_f for an initial guess that point us in the direction of a convergent numerical solution is included in Table 4.1.

TABLE 4.1: Results of $(Re_x)^{\frac{1}{2}}C_f$ when $\gamma = \pi/3$

ϕ_1	ϕ_2	M	n	K	$(Re_x)^{\frac{1}{2}}C_f$	I_f
0.1	0.1	2.0	2.0	1.0	-2.644797	[-1.0, 0.8]
0.2					-2.457452	[-1.0, 0.8]
0.3					-2.256823	[-1.0, 0.5]
0.4					-2.051066	[-1.0, 0.7]
	0.2				-2.583704	[-1.0, 0.5]
	0.3				-2.450344	[-1.0, 0.3]
	0.4				-2.266126	[-1.0, 0.3]
		2.5			-2.713690	[-1.0, 0.5]
		3.0			-2.780913	[-1.0, 0.3]
		3.5			-2.846573	[-1.0, 0.5]
			2.5		-2.803630	[-1.0, 0.4]
			3.0		-2.953928	[-1.0, 0.5]
			3.5		-3.096941	[-1.0, 0.1]
				1.5	-2.800148	[-1.0, 0.8]
				2.0	-2.947443	[-1.0, 0.8]
				2.5	-3.087776	[-1.0, 0.5]

4.5.2 Local Nusselt Number

In Table 4.2, the effects of several dimensionless parameters on the local Nusselt number is covered in detail. From the table, the following observation has been made.

- Due to a rising Eckert number, the Nusselt number exhibits a declining behaviour.
- The Nusselt number drops as the values of the magnetic parameter grow.
- The Nusselt number rises as the values of the radiation parameters do.
- Due to a rise in the Prondtl number, the Nusselt number exhibits a modest increase.
- An abrupt decrement is noticed in Nusselt number due to minner increment in the nanoparticle volume fraction.
- Nusselt number somewhat decreases as heat generating parameter increases.

The I_θ in Table 4.2 is the interval for initial guesses that direct us toward a convergent numerical solution.

TABLE 4.2: Results of $-(Re_x)^{\frac{-1}{2}} Nu_x$ when $\gamma = \pi/3$, $n = 2.0$, $K = 1.0$

Ec	M	R	Pr	ϕ_1	Q	ϕ_2	$-(Re_x)^{\frac{-1}{2}} Nu_x$	I_θ
0.4	2.0	0.1	6.2	0.1	0.1	0.1	1.928239	[-1.7, 0.7]
0.5							1.206224	[-1.5, 0.7]
0.6							0.484208	[-0.7, 0.7]
0.7							-0.237807	[-0.7, 0.7]
	2.5						1.804006	[-0.8, 0.6]
	3.0						1.681066	[-0.7, 0.7]
	3.5						1.559417	[-0.7, 0.7]
		0.2					2.082397	[-0.8, 0.7]
		0.3					2.229345	[-1.1, 0.7]
		0.4					2.370025	[-0.7, 0.7]
			6.6				1.964722	[-0.7, 0.7]
			7.0				1.998955	[-0.7, 0.7]
			7.4				2.031164	[-0.7, 0.7]
				0.2			1.223656	[-0.7, 0.7]
				0.3			0.514362	[-0.7, 0.7]
				0.4			-0.282648	[-0.7, 0.7]
					0.2		1.782450	[-0.7, 0.7]
					0.3		1.629594	[-0.7, 0.7]
					0.4		1.468571	[-0.7, 0.7]
						0.2	0.918531	[-0.8, 0.7]
						0.3	-0.436449	[-0.7, 0.7]
						0.4	-2.400721	[-0.8, 0.7]

4.5.3 Velocity Profile

The effect of permeability parameter on the velocity profile is depicted in Figure 4.1. From the graph, it can be seen that due to a slight increment in the value of K, the velocity profile behaves opositly. This occurs because a rise in K amplifies

the porous layer and consequently thins the momentum boundary layer.

The effect of the magnetic parameter is exbited in figures 4.2. The velocity profile declines with increasing values of M. It's interesting to note that a stronger magnetic force increases the flow resistance of a nanofluid. The velocity profile shrinks, which decreases the thickness of the momentum boundary layer.

The velocity profile grows as the values of nanoparticle volume fraction ϕ_1 and ϕ_2 are increased, as can be seen through Figures 4.3 and 4.4. Physically speaking, it means that as the volume fraction of nanoparticles increases, the flow is weakened and the thickness of the momentum boundary layer decreases.

Figure 4.5 shows the relationship between velocity profile and the inclined magnetic angle. From graph it is clear that the inclined magnetic angle in inversally proportion to that of velocity profile. Physically, as the inclination angle decreases, the Lorentz forces decreases. This causes the velocity profile to rise.

The effect of nonlinear stretching parameter on the velocity distribution can be seen in figure 4.6. The velocity distribution has an increasing trend by increasing the values of n. Larger values of n are what cause this increase in the non-dimensional stretching velocity, which tends to cause more deformation in the liquid. This phenomena demonstrates that as the values of n increase, the related momentum boundary layers become thicker.

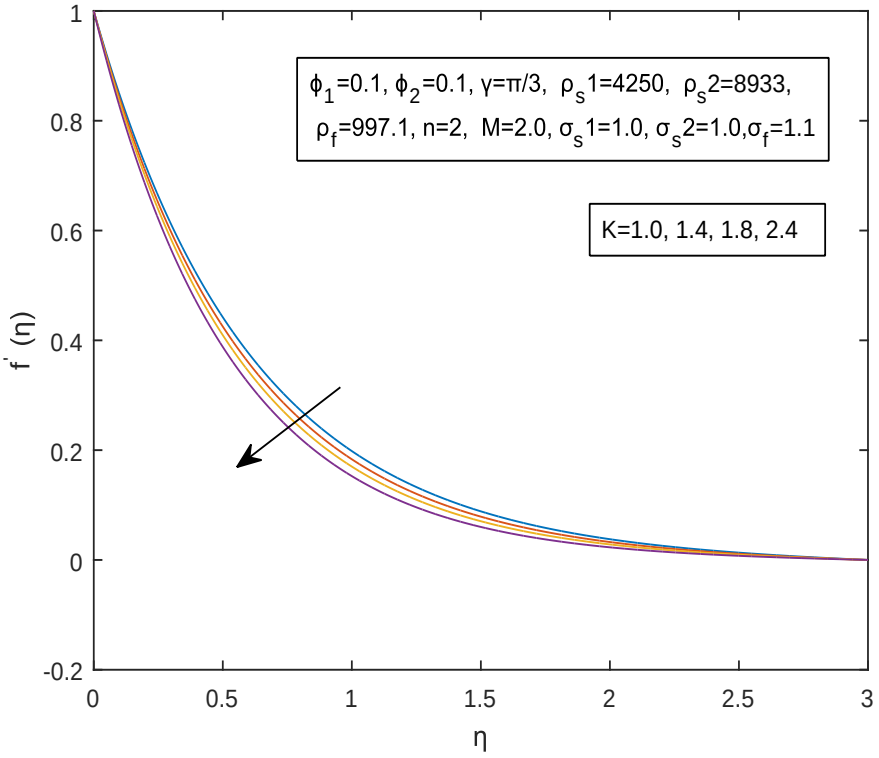

FIGURE 4.1: Influence of K on the velocity profile

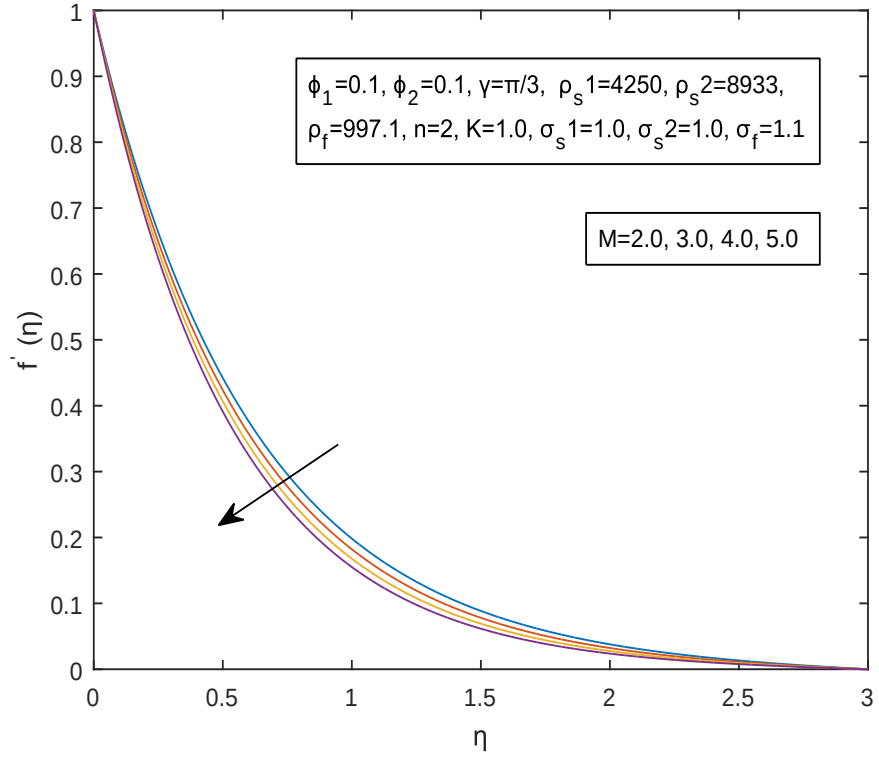

FIGURE 4.2: Influence of M on the velocity profile.

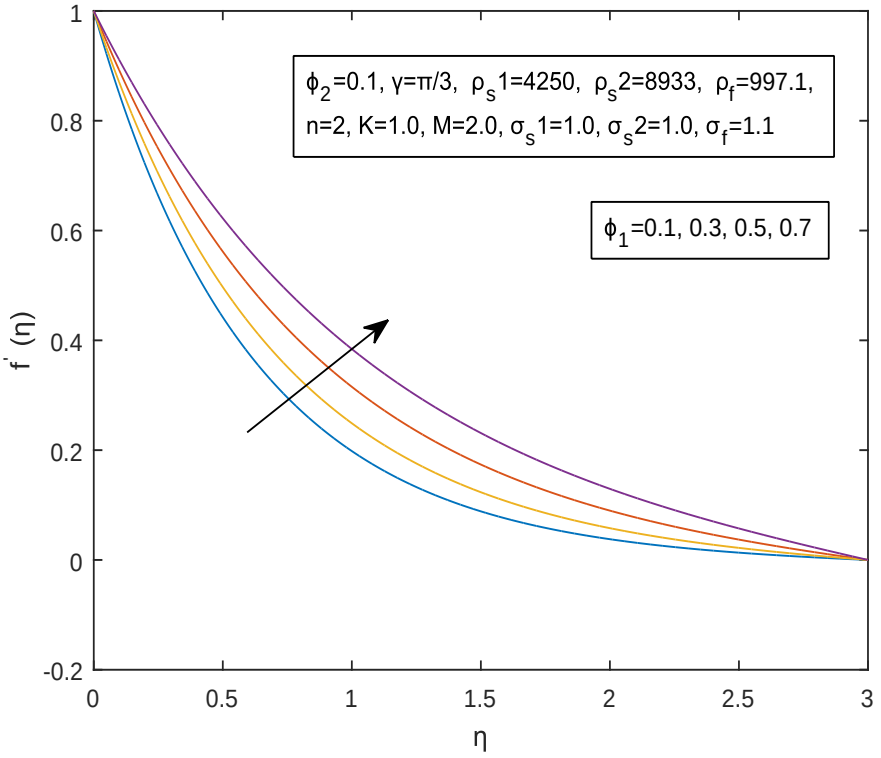

FIGURE 4.3: Influence of ϕ_1 on the velocity profile.

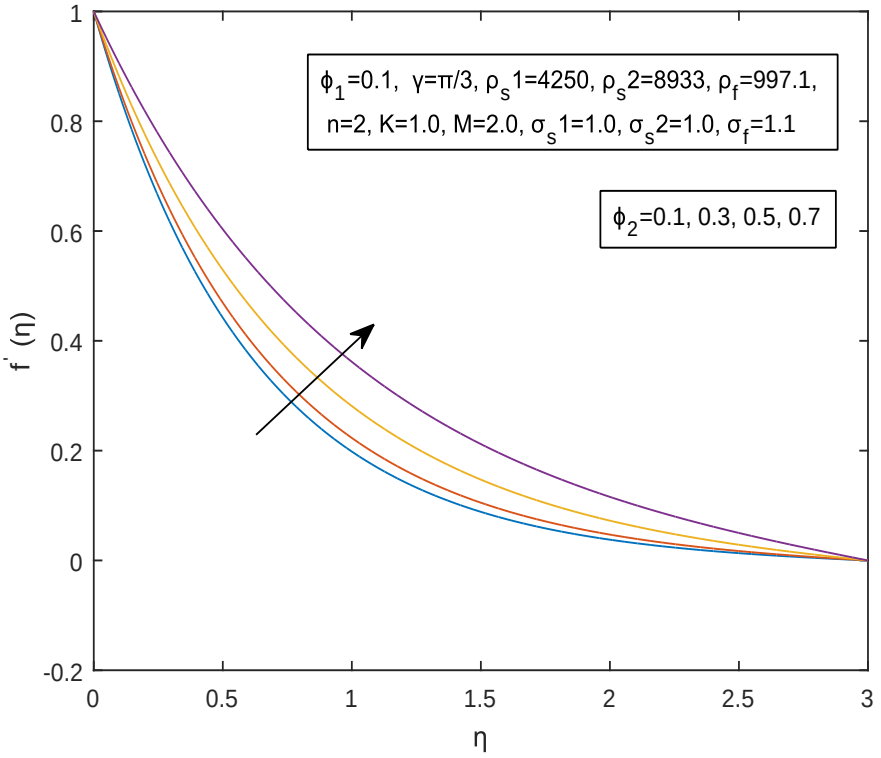

FIGURE 4.4: Influence of ϕ_2 on the velocity profile.

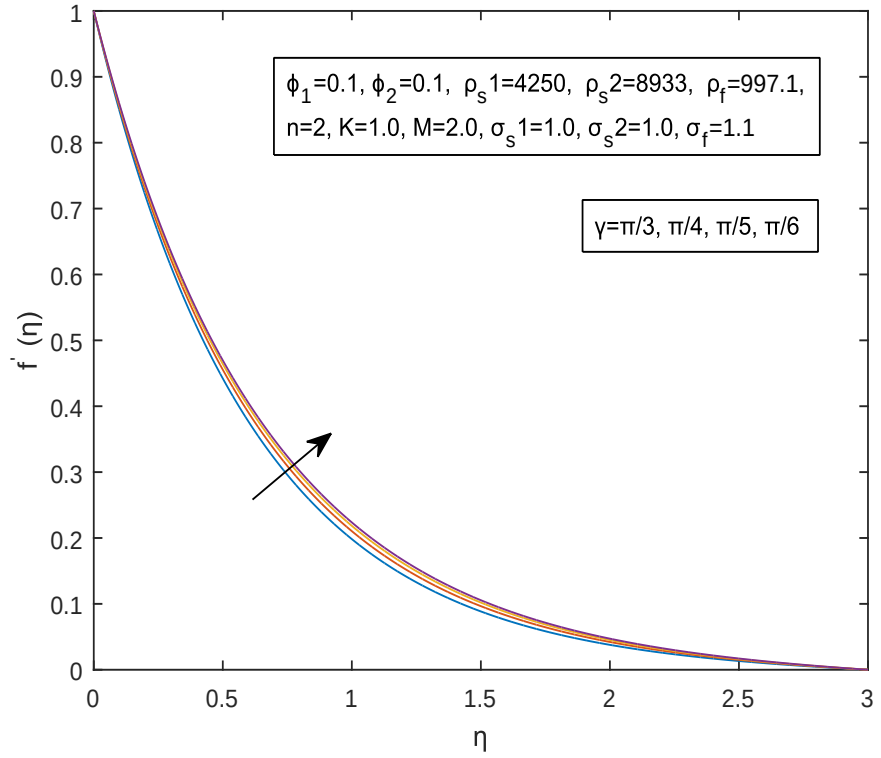

FIGURE 4.5: Influence of γ on the velocity profile.

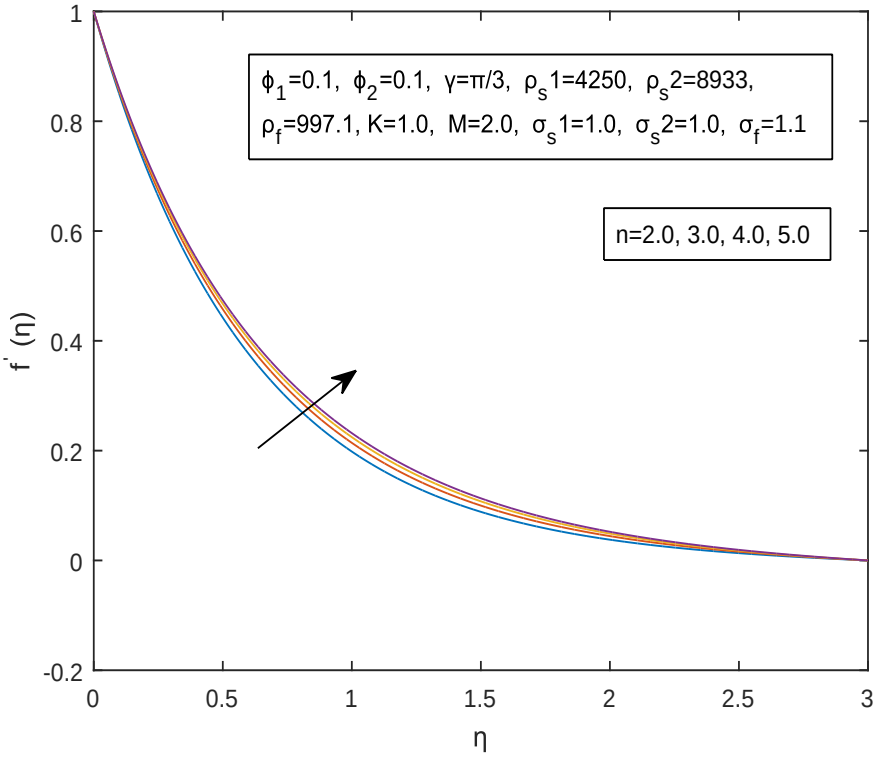

FIGURE 4.6: Influence of n on the velocity profile.

4.5.4 Temperature Profile

The effect of the magnetic parameter on the temperature profile is depicted in Figure 4.7. The temperature profile grows with increasing values of M. Physically, when M increases, the Lorentz force in the magnetic field gets greater, increasing the thickness of the thermal boundary layer.

Figures 4.8 and 4.9 display the impact of ϕ_1 and ϕ_2 on the temperature distribution. By rising the values of ϕ_1 and ϕ_2 the temperature distribution show the increasing behavior.

The temperature distribution for decreasing values of inclination angle shows decreasing behaviour and this phenomenon can be seen in Figure 4.10. Physically, decreasing the angle of inclination increases the Lorentz force, which produces more heat and lowers the temperature profile.

The effect of nonlinear stretching parameter on temperature distribution is seen in Figure 4.11. The temperature distribution is lowered as n is increased.

The effect of the radiation parameter on the temperature distribution is depicted in Figure 4.12. The temperature distribution is improved by raising the values of R. Greater values of the radiation parameter add more heat to the system, which eventually raises the fluid's temperature and thickens the thermal boundary layer.

Figure 4.13, shows the impact of the Prandtl number on the temperature distributions. Since Pr is directly proportionate to the viscous diffusion rate and inversely related to the thermal diffusivity, so the thermal diffusion rate suffers a reduction for the larger values of Pr and subsequently, the temperature of the fluid drops significantly. Moreover, a decrement in the thermal boundary layer thickness has been noted.

The impact of heat generation on the temperature profile can be seen in Figure 4.14. It is observed that for an increasing values of Q more heat is generated, because of this temperature and thermal boundary layer thickness increases.

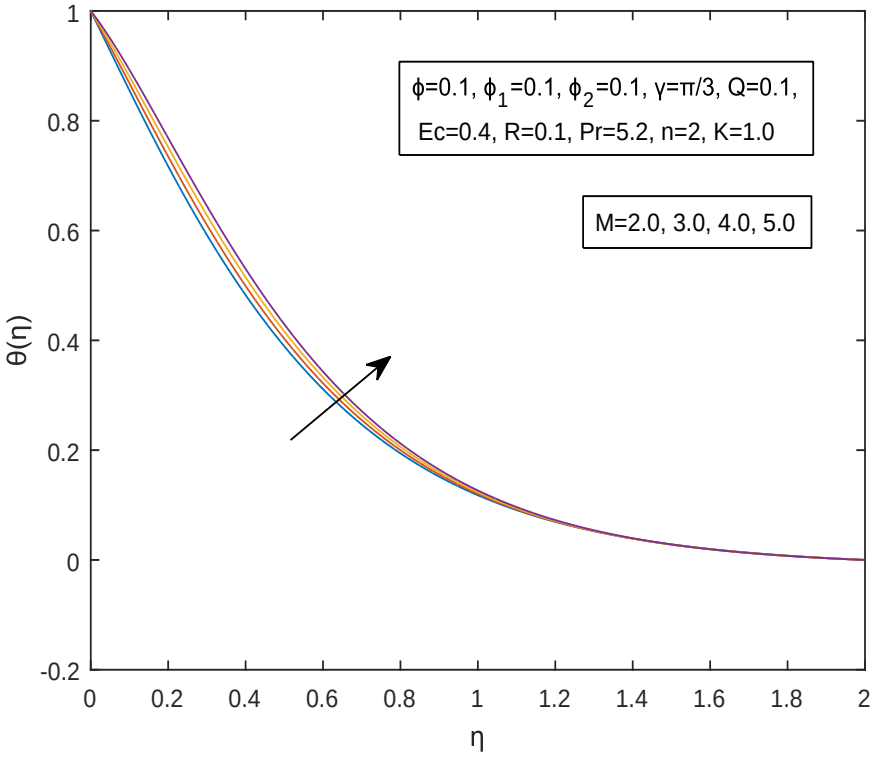

FIGURE 4.7: Impact of M on the temperature profile.

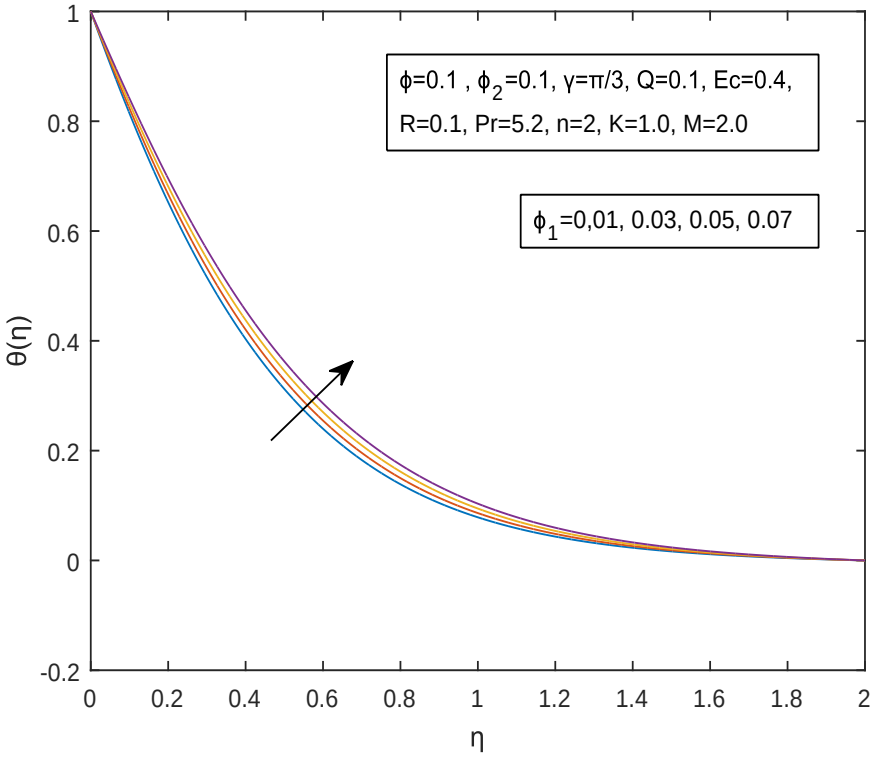

FIGURE 4.8: Impact of ϕ_1 on the temperature profile.

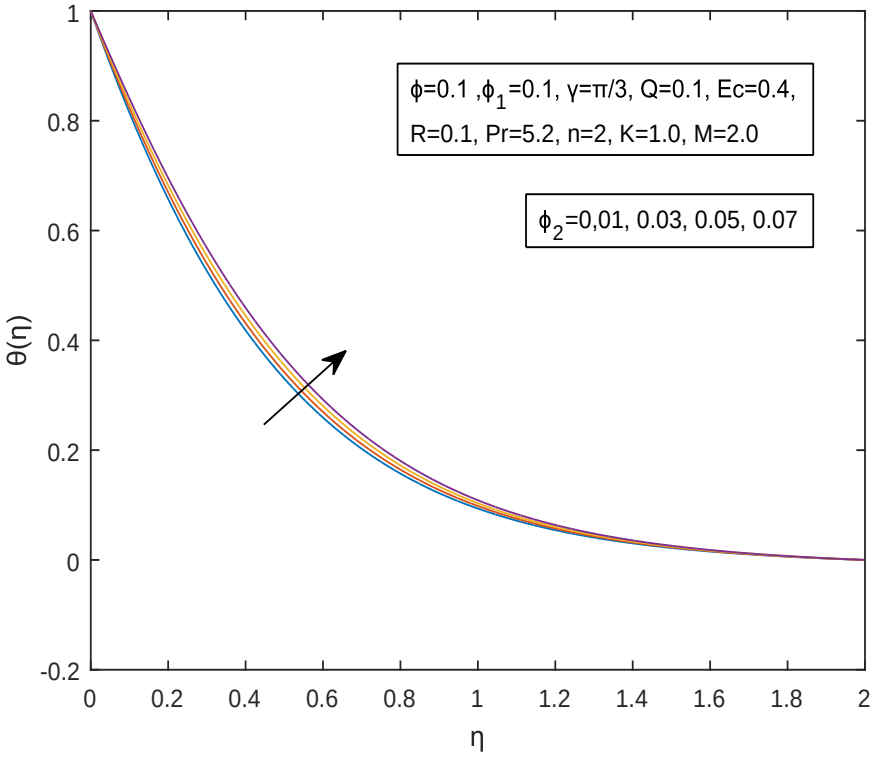

FIGURE 4.9: Impact of ϕ_2 on the temperature profile.

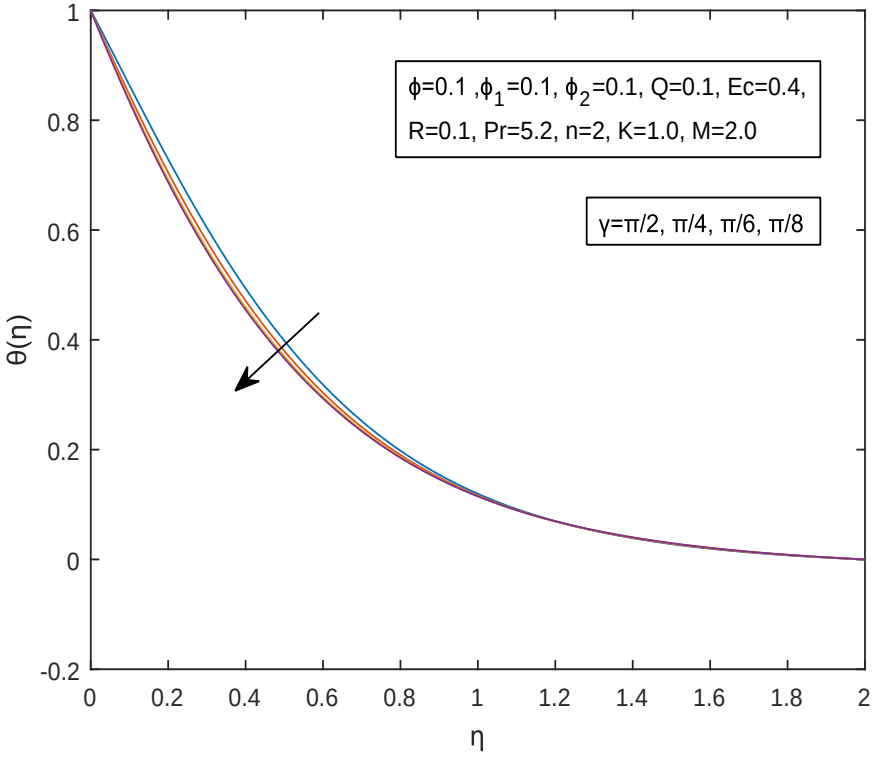

FIGURE 4.10: Impact of γ on the temperature profile.

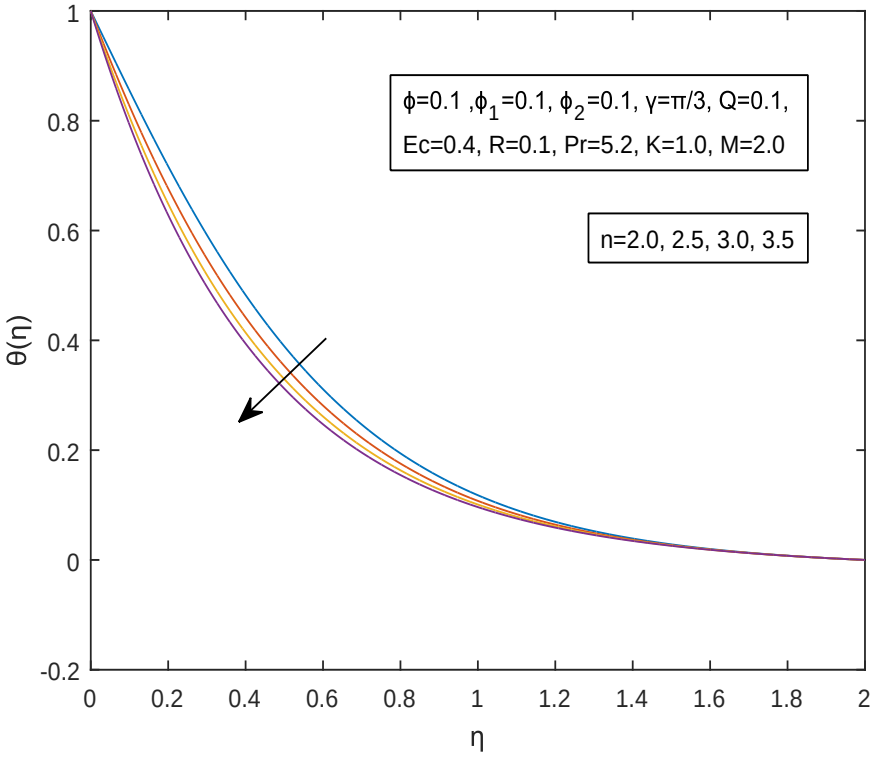

FIGURE 4.11: Impact of n on the temperature profile.

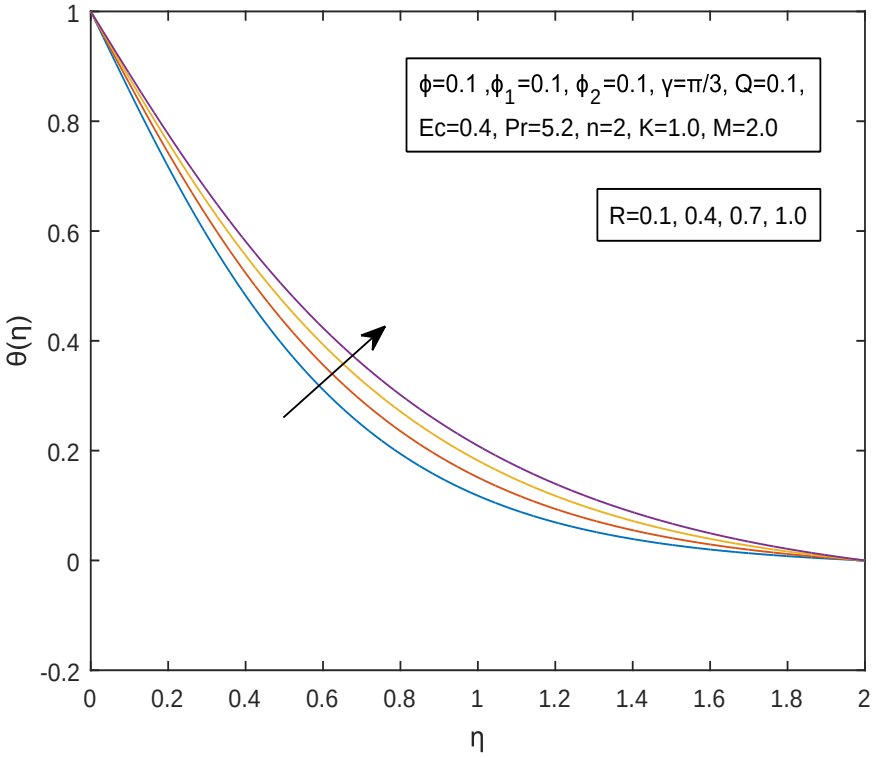

FIGURE 4.12: Impact of R on the temperature profile.

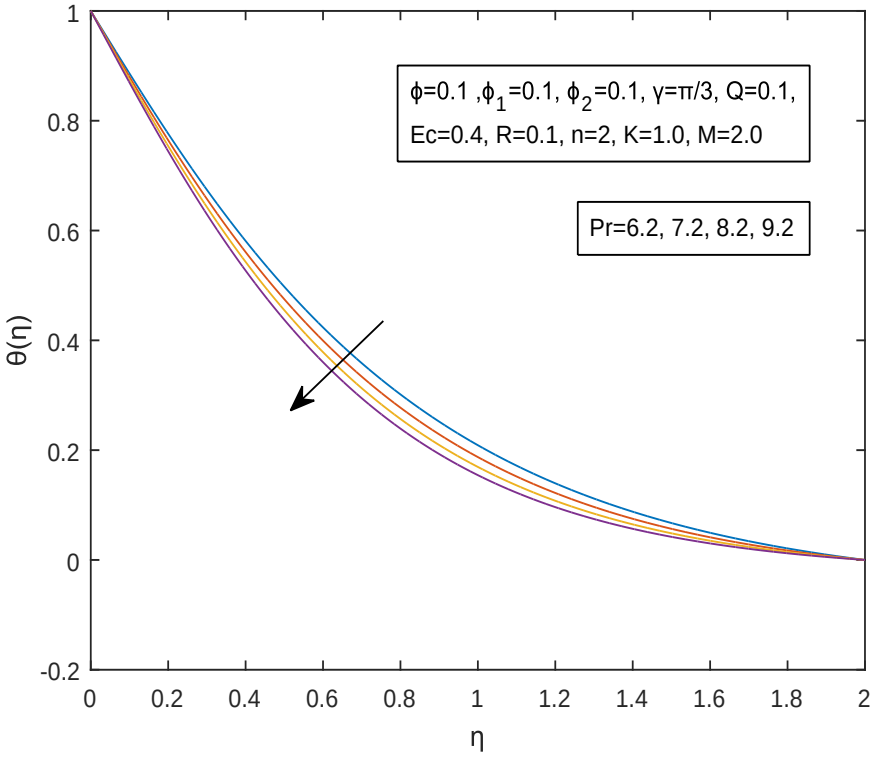

FIGURE 4.13: Impact of Pr on the temperature profile.

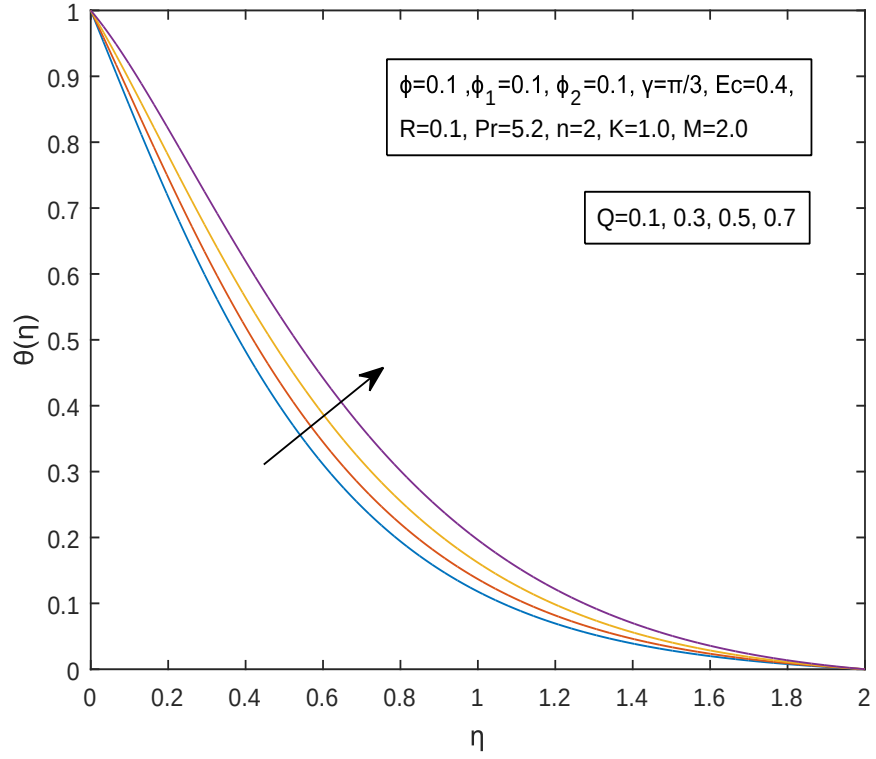

FIGURE 4.14: Impact of Q on the temperature profile.

Chapter 5

Conclusion

In this thesis, Jafar et al [25] work is examined and expanded on in light of the impact of an inclined magnetic field and hybrid nanofluid. First of all, using appropriate similarity transformations, momentum and energy equations are transformed into ODEs. Numerical solutions to the modified ODEs have been discovered using the shooting technique. The results are presented as tables and graphs for velocity, temperature profiles as well as for skin friction cofficient and Local Nusselt number using various values of the governing physical parameters. The following is the summary of the present research:

- The velocity profile falls as the permeability parameter K values rise, whereas the temperature profile rises.
- The velocity profile decreases while the temperature distribution increases, as the magnetic parameter M increases.
- Both the velocity and temperature profile rise with the rising values of ϕ_1 and $\phi 2$.
- The velocity profile shows an increasing behaviour as a result of decreasing values for inclined magnetic angle γ.
- The decreasing values of inclined magnetic angle γ cause a decrease in the Nusselt number.

- While increasing the values of nonlinear stretching parameter n causes a decrease in the temperature profile but an increase in the skin friction coffi-cient.
- The temperature profile decreases as the Prondtl number Pr increases.
- The numerical values of the temperature profile $\theta(\eta)$ are raised as a result of the ascending values of radiation parameter R.
- Due to the ascending values of heat generation parameter Q, the value of Local Nusselt number Nu_x is increased.

Bibliography

[1] Y. Cengel, J. Cimbala, and R. Turner, *EBOOK: Fundamentals of Thermal-Fluid Sciences (SI units)*. McGraw Hill, 2012.

[2] B. Xia and D.-W. Sun, "Applications of Computational Fluid Dynamics (CFD) in the Food Industry: A Review," *Computers and Electronics in Agriculture*, vol. 34, no. 1-3, pp. 5–24, 2002.

[3] R. Dash, K. Mehta, and G. Jayaraman, "Casson fluid flow in a pipe filled with a homogeneous porous medium," *International Journal of Engineering Science*, vol. 34, no. 10, pp. 1145–1156, 1996.

[4] S. U. Choi, "Nanofluid Technology: Current status and future research," tech. rep., Argonne National Lab.(ANL), Argonne, IL (United States), 1998.

[5] J. Buongiorno, "Convective Transport in Nanofluids," 2006.

[6] R. K. Tiwari and M. K. Das, "Heat transfer augmentation in a two-sided lid-driven differentially heated square cavity utilizing nanofluids," *International Journal of heat and Mass transfer*, vol. 50, no. 9-10, pp. 2002–2018, 2007.

[7] J.-C. Yang, F.-C. Li, W.-W. Zhou, Y.-R. He, and B.-C. Jiang, "Experimental investigation on the thermal conductivity and shear viscosity of viscoelastic-fluid-based nanofluids," *International Journal of Heat and Mass Transfer*, vol. 55, no. 11-12, pp. 3160–3166, 2012.

[8] W. Khan and I. Pop, "Boundary-layer flow of a nanofluid past a stretching sheet," *International journal of heat and mass transfer*, vol. 53, no. 11-12, pp. 2477–2483, 2010.

[9] P. Rana and R. Bhargava, "Finite element simulation of transport phenomena of viscoelastic nanofluid over a stretching sheet with energy dissipation," *Journal of Information and Operations Management*, vol. 3, no. 1, 2012.

[10] H. Alfvén, "Existence of electromagnetic-hydrodynamic waves," *Nature*, vol. 150, no. 3805, pp. 405–406, 1942.

[11] I. Mbeledogu and A. Ogulu, "Heat and Mass transfer of an unsteady MHD natural convection flow of a rotating fluid past a vertical porous flat plate in the presence of radiative heat transfer," *International Journal of Heat and Mass Transfer*, vol. 50, no. 9-10, pp. 1902–1908, 2007.

[12] D. Chauhan and R. Agrawal, "MHD flow and heat transfer in a channel bounded by a shrinking sheet and a plate with a porous substrate," *Journal of Engineering Physics and Thermophysics*, vol. 84, no. 5, pp. 1034–1046, 2011.

[13] M. E. Yazdi, A. Moradi, and S. Dinarvand, "MHD mixed convection stagnation-point flow over a stretching vertical plate in porous medium filled with a nanofluid in the presence of thermal radiation," *Arabian Journal for Science and Engineering*, vol. 39, no. 3, pp. 2251–2261, 2014.

[14] J. Sarkar, P. Ghosh, and A. Adil, "A Review on Hybrid Nanofluids: Recent Research, Development and Applications," *Renewable and Sustainable Energy Reviews*, vol. 43, pp. 164–177, 2015.

[15] N. Acharya, R. Bag, and P. K. Kundu, "On the impact of nonlinear thermal radiation on magnetized hybrid condensed nanofluid flow over a permeable texture," *Applied Nanoscience*, vol. 10, no. 5, pp. 1679–1691, 2020.

[16] N. Acharya, "On the flow patterns and thermal behaviour of hybrid nanofluid flow inside a microchannel in presence of radiative solar energy," *Journal of Thermal Analysis and Calorimetry*, vol. 141, no. 4, pp. 1425–1442, 2020.

[17] N. Acharya, S. Maity, and P. K. Kundu, "Framing the hydrothermal features of magnetized $tio_2 - -cofe_2o_4$ water-based steady hybrid nanofluid flow

over a radiative revolving disk," *Multidiscipline Modeling in Materials and Structures*, 2019.

[18] S. G. Bejawada, Y. D. Reddy, W. Jamshed, K. S. Nisar, A. N. Alharbi, and R. Chouikh, "Radiation effect on MHD Casson fluid flow over an inclined non-linear surface with chemical reaction in a forchheimer porous medium," *Alexandria Engineering Journal*, vol. 61, no. 10, pp. 8207–8220, 2022.

[19] A. J. Chamkha, C. Issa, and K. Khanafer, "Natural convection from an inclined plate embedded in a variable porosity porous medium due to solar radiation," *International Journal of Thermal Sciences*, vol. 41, no. 1, pp. 73–81, 2002.

[20] N. Hadidi, R. Bennacer, and Y. Ould-Amer, "Two-dimensional thermosolutal natural convective heat and mass transfer in a bi-layered and inclined porous enclosure," *Energy*, vol. 93, pp. 2582–2592, 2015.

[21] S. U. Devi and S. A. Devi, "Heat transfer enhancement of cu-$al\_\{2\}o\_\{3\}$/water hybrid nanofluid flow over a stretching sheet," *Journal of the Nigerian Mathematical Society*, vol. 36, no. 2, pp. 419–433, 2017.

[22] T. Dang, J.-t. Teng, J.-c. Chu, T. Xu, S. Huang, S. Jin, and J. Zheng, "Single-phase heat transfer and fluid flow phenomena of microchannel heat exchangers," *Heat Exchangers: Basics Design Applications*, p. 249, 2012.

[23] S. K. Das, S. U. Choi, W. Yu, and T. Pradeep, *Nanofluids: science and technology*. John Wiley & Sons, 2007.

[24] M. Zaydan, A. Wakif, I. Animasaun, U. Khan, D. Baleanu, and R. Sehaqui, "Significances of blowing and suction processes on the occurrence of thermo-magneto-convection phenomenon in a narrow nanofluidic medium: a revised buongiorno's nanofluid model," *Case Studies in Thermal Engineering*, vol. 22, p. 100726, 2020.

[25] A. B. Jafar, S. Shafie, and I. Ullah, "MHD radiative nanofluid flow induced by a nonlinear stretching sheet in a porous medium," *Heliyon*, vol. 6, no. 6, p. e04201, 2020.

[26] R. W. Fox, A. T. McDonald, and J. W. Mitchell, *Fox and McDonald's introduction to fluid mechanics*. John Wiley & Sons, 2020.

[27] R. Bansal, *A Textbook of Fluid Mechanics*. Firewall Media, 2005.

[28] J. A. Schetz and A. E. Fuhs, *Fundamentals of fluid mechanics*. John Wiley & Sons, 1999.

[29] R. Bansal, *A Textbook of Fluid Mechanics and Dydraulic Machines*. Laxmi publications, 2004.

[30] D. L. Logan, *A First Course in the Finite Element Method*. Cengage Learning, 2016.

[31] J. Ahmed and M. S. Rahman, *Handbook of Food Process Design*. John Wiley & Sons, 2012.

[32] P. A. Davidson and A. Thess, *Magnetohydrodynamics*, vol. 418. Springer Science & Business Media, 2002.

[33] R. W. Fox, A. McDonald, and P. Pitchard, *Introduction to Fluid Mechanics*. John Wiley & Sons, Inc, 2006.

[34] J. N. Reddy and D. K. Gartling, *The Finite Element Method in Heat Transfer and Fluid Dynamics*. CRC press, 2010.

[35] J. Kunes, *Dimensionless physical quantities in science and engineering*. Elsevier, 2012.

[36] M. Hamad and M. Ferdows, "Similarity solutions to viscous flow and heat transfer of nanofluid over nonlinearly stretching sheet," *Applied Mathematics and Mechanics*, vol. 33, no. 7, pp. 923–930, 2012.

[37] M. Sheikholeslami, M. Hatami, and D. Ganji, "Nanofluid flow and heat transfer in a rotating system in the presence of a magnetic field," *Journal of Molecular Liquids*, vol. 190, pp. 112–120, 2014.

[38] M. Arshad, A. Hussain, S. A. G. A. Shah, P. Wróblewski, M. A. Elkotb, M. A. Abdelmohimen, A. Hassan, *et al.*, "Thermal energy investigation of magnetohydrodynamic nano-material liquid flow over a stretching sheet: comparison of single and composite particles," *Alexandria Engineering Journal*, vol. 61, no. 12, pp. 10453–10462, 2022.